Project Report
TIP-192

Predictive Analytics for Wide Area Search and Rescue (PAWSAR): FY23 HADR Technical Investment Program

C. L. Council
D. W. Schuldt
J. Liu

15 December 2023

Lincoln Laboratory
MASSACHUSETTS INSTITUTE OF TECHNOLOGY
LEXINGTON, MASSACHUSETTS

This material is based upon work supported by the Department of the Air Force under Air Force Contract No. FA8702-15-D-0001.

This report is the result of studies performed at Lincoln Laboratory, a federally funded research and development center operated by Massachusetts Institute of Technology. This material is based upon work supported by the Department of the Air Force under Air Force Contract No. FA8702-15-D-0001. Any opinions, findings, conclusions or recommendations expressed in this material are those of the author(s) and do not necessarily reflect the views of the Department of the Air Force.

Massachusetts Institute of Technology
Lincoln Laboratory

Predictive Analytics for Wide Area Search and Rescue (PAWSAR): FY23 HADR Technical Investment Program

C. L. Council
D. W. Schuldt
J. Liu
Group 21

Project Report TIP-192
15 December 2023

This material is based upon work supported by the Department of the Air Force under Air Force Contract No. FA8702-15-D-0001.

Lexington Massachusetts

This page intentionally left blank.

EXECUTIVE SUMMARY

When a disaster such as a hurricane strikes a large geographic area, specially trained urban search and rescue (USAR) teams may conduct a wide area search, looking for an unknown number of people within an unclear boundary. Allocating the right number of USAR teams to a response, identifying where they should search, and how to subdivide the search area are tasks performed by experienced personnel. In this paper, we describe an effort to establish a predictive analytics framework that can provide these decision makers with a quantified understanding of potential impacts, time, and resources required to conduct searches within a given area, and how an urban area may be best divided into subareas of equal work.

Using data collected by USAR teams from past hurricane responses, we develop prototype models that 1) estimate structural damage based on other hurricane predictive models, 2) estimate the time required to search structures with a set of damage distributions, and 3) partition a city into areas of equal work. We demonstrate how these models can be used in a prototype operational pipeline that could be executed in sync with the USAR operational cycle.

Future work entails validation of the models against future hurricane impacts and expanding the city partitioning algorithm to derive work estimation from the modeled damage and search time predictions.

Numerous supporting analyses conducted as part of this work have also yielded insights into how USAR teams conduct wide area search operations. These insights may be immediately applicable to the community's perpetual continuous improvement model.

This page intentionally left blank.

ACKNOWLEDGEMENTS

This work was funded by MIT Lincoln Laboratory from 2021 to 2023. During that time, numerous MIT LL staff have contributed to the project both formally and informally. Listed alphabetically they are:

John Aldridge, Rajmonda Caceres, Kendrick Cancio, Chad Council, Consuelo Cuevas, Grace Kessenich, Jeff Liu, and Dieter Schuldt.

In addition, the team received data, periodic feedback, and guidance from the USAR community, including:

- National Search and Rescue Geospatial Coordination Group
- National Alliance for Public Safety GIS
- FEMA Urban Search & Rescue
- FEMA Response Geospatial Office
- State Urban Search and Rescue

This page intentionally left blank.

TABLE OF CONTENTS

TABLE OF CONTENTS
(Continued)

Page

LIST OF ILLUSTRATIONS

LIST OF ILLUSTRATIONS
(Continued)

LIST OF ILLUSTRATIONS
(Continued)

This page intentionally left blank.

LIST OF TABLES

This page intentionally left blank.

1. INTRODUCTION

The number one priority in disaster response is life safety (Federal Emergency Management Agency, 2018). This is an exceptional challenge during major disasters such as hurricanes where the damage is widespread. Often, the public safety infrastructure responsible for the life safety of the community is either incapacitated by damage from the disaster or overwhelmed by the size and scope of the disaster. Under these conditions, outside support to life safety is provided by specially trained Urban Search and Rescue Teams (USAR).

In order to support life safety after a hurricane, USAR teams conduct a Wide Area Search to identify damage and locate survivors. Wide Area Search is defined as the search for an unknown number of people across an area with uncertain boundaries. This is the type of environment encountered in the immediate aftermath of a hurricane.

One of the most important decisions that can be made right after a disaster is how many USAR teams are needed in the response. The USAR teams which respond to hurricanes are located across the country and their travel time to the disaster location can be considerable. The Federal Emergency Management Agency (FEMA) supports and maintains the National Urban Search and Rescue Response System (US&R), which consists of 28 teams available for federal employment during disasters. Many states also maintain USAR teams trained and equipped to similar standards as the FEMA US&R teams. The state run USAR teams may provide aid within their own state or to other states when requested. Calling in too many teams results in cost overruns that are passed on to the tax payer. If too few USAR teams are brought in, however, then people who could potentially be saved may perish (or at the least wait longer than they would have had to). An effective strategy has been to borrow from the insights gained before the disaster and adapt them in light of information acquired immediately before, during, and after the disaster.

While every disaster response is different, a typical USAR approach to a Wide Area Search consists of an iterative set of defined search types:

- Recon: preliminary survey to determine scope and magnitude. This may be conducted by vehicle, either on the ground or from the air.
- Hasty Search: Fast and methodical search for immediate rescues of survivors who are readily accessible without significant extrication effort.
- Primary Search: an exterior search of each structure in an area. The specific methods will vary by disaster and requirements defined as rules of engagement by the local authority having jurisdiction, if available. Search methods may include knocking on doors, looking in windows, hailing, circling every structure looking for signs that warrant further search or survivor interaction.

- Secondary Low Search: Systematic search of every room of every structure. For example, a neighborhood that experienced over six feet of flood waters and the water has receded, the search would be looking inside those structures for incapacitated survivors or deceased victims.
- Secondary High Search: Delayering of debris from a collapsed structure.
- Targeted Search: A specific location to search based on reliable information. For example, a 911 call that could not be responded to during the hurricane.

A textbook USAR Wide Area Search response would start with a Recon Search to bound the area, followed by a Hasty search of priority areas identified during the Recon, and then a Primary search to account for all structures in the area. In reality, each search type may be ongoing simultaneously in different geographic areas.

One could frame this completely as an optimization problem that aims to minimize the overall cost, but because of the human aspects involved in this scenario we have elected to instead provide a suite of tools that emergency managers can use to make a decision that meets their various (and potentially vague) criteria. Placing a value on a human life is very difficult, even for seasoned disaster management professionals, so coming up with all of the parameters necessary to generate an optimal solution may not be possible. There are also other factors that may not be easily quantified, that go into the decision process.

Part of determining the number of teams required is understanding how long it is expected for a given set of searchers to complete their tasking. To get the best outcome, the tools developed here divide the space into an efficient partition that enables the fastest search of the region. Current methodologies give broad latitude to the mission commander to select the region to which each team is assigned, but with geographic computation we are able to construct regions that ensure a more balanced distribution of resources.

For most disasters the local search and rescue teams are adequate for the response. As such, this work focuses on large area disasters that require a substantial response from a number of partner agencies. In general, this means that the disasters in question will be hurricanes, which affect thousands of square miles, and potentially millions of people.

To illustrate the size, scope, and magnitude of hurricane impacts that necessitate Wide Area Searches conducted by USAR, we look at the data collected during hurricanes Laura (2020), Delta (2020), Ida (2021), and Ian (2022). The typical geographic scope of areas searched by USAR ranges from 2,000 to 4,000 square miles, but particularly devastating storms can range over 10,000 (Ida) square miles or more. The number of structures searched in the aftermath of these events ranges from 28,000 to 108,000 (Ian) structures searched.

Based on FEMA US&R Deployment data available for the ten-year period between 2010 and 2020, there have been 39 events with FEMA activations or deployments. Based on the number of teams of each type for each event, and the number of people per type of team, this equates to 13,426 people deployed over

that ten-year span. The average deployment consists of 345 people, with some events requiring well over 1,000 search and rescue personnel.

Emergency managers at the state and federal level are faced with a significant challenge for hurricanes: Prior to landfall, they must be certain that they have enough resources to support life safety in place, without excessively tying up the sparse and costly resource of additional USAR teams. This decision process is based on hurricane forecast data with some uncertainty, and requires multiple days of travel time for outside USAR resources to be positioned.

After hurricane landfall, the next significant challenge involves those USAR teams organizing and coordinating hundreds of search and rescue personnel to search tens of thousands of structures spread out over thousands of square miles under austere conditions with significant time pressure.

Because the size and scope of impacts isn't known for certain ahead of time, it may take days of Recon efforts to determine that they don't have enough resources, and those resources will then be multiple days away, delaying aid to survivors.

This page intentionally left blank.

2. DATA AND METHODOLOGY

The FEMA Urban Search and Rescue system originally established a standardized set of data to collect during disasters in 2014 as part of a system named Iron Sights. The standard data set was also adopted by many state USAR teams over time. As technology for field data collection evolved, both FEMA and state USAR teams migrated to a smartphone-based field data collection system that exists within the ecosystem developed by Esri. This new system is known as SARCOP and has been adopted by numerous search and rescue teams across the United States (Collins, n.d.).

The data collected within the SARCOP system consists of several different categories of information, including interactions with people (e.g., rescues or assists) and damage observations. The data we focused on was the assessments of structure damage by USAR teams. Per the current data dictionary, a USAR team member may record a data point for each structure searched and classify the damage observed as one of six classes of damage: (National Alliance for Public Safety GIS, 2023).

Damage Observations		
	Unaffected	No visible or reported damage.
	Affected	Damage to the structure is mostly cosmetic.
	Minor	Repairable non-structural damage.
	Major	Structural damage or other significant damage that requires extensive repairs.
	Destroyed	The structure is a total loss.
	Unknown	The status of the structure is unknown.

The current, full data dictionary is included as Appendix D: SARCOP Data Dictionary.

Our initial effort consisted of several exploratory analyses of this data to determine the quality of the data, what sort of patterns may exist, operational insights that may be derived from those patterns, and ultimately, how could this data be used to support resource allocation of USAR teams for very large wide area searches. Our hypothesis was that each type of interaction performed by a member of a search and rescue team had some impact on the time it took for them to perform their duties in an area. For example, an undamaged house would take a different amount of time to "clear" of any people than a house that had suffered major damage.

The field data collection technology evolved over time, varying the data dictionary, schema, and storage formats, making it impractical to analyze older data in the same context as more recently collected data. The team focused on several large USAR deployments from 2020 to 2022.

The data collected by USAR teams consists of several pieces of supporting information in addition to the observation itself: the location where it was recorded, which team or squad recorded the data, and the date and time the data was recorded. This provides the potential for a very valuable spatiotemporal data set describing what the USAR team did and what they encountered over time. Unfortunately, operational realities of conducting search and rescue in a disaster environment make it challenging to collect high fidelity data that represents exactly what happened and where. It may be impossible, for example, for a squad to create a data observation for each structure at the exact time that search is conducted, and data maybe be collected in batches making the temporal nature less granular.

3. EXPLORATORY ANALYSES

The first effort was to clean the available data, eliminating obvious outliers such as data recorded at the USAR team's home base, or data that had been mixed in from a previous disaster. This process was performed for data collected during Hurricane Laura (2020), Hurricane Delta (2020), and Hurricane Ida (2021). Numerous exploratory analyses were then conducted to explore the data and identify patterns that may exist in the data. The details of these analyses are in Appendix A: Exploratory Analyses.

The analyses of the data for these hurricanes illuminated the following observations, which added confidence that the data could be used to represent aspects of the operations.

- Areas searched by squads show signs of significant overlap, indicating possible duplication of effort or assignments that result in inefficient travel.
- Looking at the time spent conducting a search of an area over the course of an incident shows that searches earlier in the response and later in the response tend to be shorter time durations than those searches that take place in the middle of the response. This could be an indicator of the type of work being done at the beginning and end of a deployment such as initial recon at the beginning of a deployment and wrapping up at the end of the deployment.
- Searches marked as "Secondary" tend to take longer than the other search types. Given the thorough nature of a secondary search, this adds confidence that the data can represent the operations.
- Recon searches tend to get faster as the operation progresses. This aligns with expectations in that the overall area to recon should continually get smaller as the response progresses over time.
- Secondary searches occasionally occur in the middle of the operation. This speaks to the complex nature of coordinating a search over a very wide area, where progress in one area may be nearing the end, culminating in secondary searches of some structures, while searches in other geographic areas may be still undergoing recon.
- There is some correlation between the total path length traveled by a squad and the number of structures searched. This supports the premise that most travel distance recorded is travel between structures.
- The final search day shows a greater distance between structures searched, driven by both fewer structures to search and longer travel distance between them.
- The path lengths increase over time, which may indicate a high topological dependance. The distance traveled is coupled to the layout of structures in an area.

- Most squads cover the same geographic area per day.
- The area covered by a squad is most variable on the first day and last day of the response.
- For Hurricane Delta, excluding travel to and from the search area, the average area searched by a squad was 1.75 square miles.
- Searches tend to start in the center of the impacted area.
- FEMA generated impact forecasts (POST/TEMPO) do have a correlation with the USAR damage observations
- Principal component analysis indicates that the hazard score in the POST/TEMPO product is an independent variable that explains variability in the damage observations.
- There are some variations in the data that indicate that the data doesn't represent the activity in perfect fidelity, such as long gaps between data recording times, or clusters of data recorded near simultaneously. These variations could be the result of user errors or the result of limitations placed on the USAR teams given the conditions of the operation. It simply may not have been possible to record each data point at the time and location where the activity occurred.
- A regression model can be generated to predict the time required to search an area based on the damage in that area, but the variation in data fidelity results in a model that underpredicts the required time.

Some of these observations are indicating conclusions that are likely very obvious to USAR members, such as secondary searches taking longer than other search types. These confirmations serve to support the idea that the data collected by USAR teams can be used to represent the activity for a response in enough detail to build further tools to support USAR operations. These insights led to the development of the overall system concept described in the next section.

4. SYSTEM CONCEPT DEVELOPMENT

Exploratory analyses of the data identified several ways that further analysis and development could support more optimal resource allocation for USAR. Specifically, it follows that:

- Breaking the work area up into well-defined and connected segments before or in the very early stages of the response will reduce overlap, duplication of effort, and inefficient travel times between search areas.
- Understanding the amount of work done by a USAR team under different conditions can help with sizing the response and efficiently assign teams to work areas.
- In order to utilize any sort work time estimate based on conditions, we must be able to forecast those conditions.

This leads to three separate analytical paths that can complement each other to form a system:

- Establish search production rates based on damage distributions.
- Determine the correlation between forecasted damage and USAR-observed damage.
- Divide an area into segments of equal production based on the expected geographic distribution of damage in the area and the corresponding production rates based on that expected damage.

Each component will be described further in the subsequent sections.

4.1 ESTABLISH PRODUCTION RATE ESTIMATES FOR DIFFERENT CONDITIONS

There are many examples of repeatable processes that have well-defined rates at which that process produces its outcome. Some examples include the rate manufacturing a good, constructing roadways, and oil and gas well output. For each of these examples, there are key attributes that need to be defined:

- Units for measuring the rate
- Conditions under which the rate is applicable

Many production rates include a range of values, from low to median to high. For example, the Wisconsin Department of Transportation has a published a production rate table (Wisoncisn Department of Transportation, n.d.) for various road construction components. Their published rate for installing Rumble Strips shows:

Table 1: Wisconsin DOT Production Rates (Modified for Clarity)

Item	Unit	Expected Production Range
Rumble Strips (Shoulder)	Linear Feet per Day	24,000–60,000 (35,000 typical)
Rumble Strips (Centerline)	Linear Feet per Day	21,000–46,000 (36,000 typical)

Note that the task of placing rumble strips has slightly different rates depending on where on the roadway the strips are installed, demonstrating how a production rate can be established for a task being performed under different conditions.

An example more germane to wide area search can be found in the US Forest Service wildfire fighting domain. The USFS has studied and developed production rates for constructing Fireline under numerous variables, including: The relevant fire behavior fuel model, specific conditions in that area, the size and type of crew or machinery being used, and the slope of the terrain. A sample production rate table is shown below, taken directly from the USFS. National Technology and Development Program, USFS, n.d.).

Table 2: Sustained Line Production Rates of 20-Person Crews in Feet per Hour*

Fire Behavior Fuel Model	Type I Direct	Type I Indirect	Type II & II IA*** Direct	Type II & II IA*** Indirect
1 Short Grass 2 Open Timber Grass	1,122 (792–1,386)**	627 (508–746)	627 (174–660)	285 (174–380)
4 Chaparral	436 (330–528)	330 (178–482)	449 (80–640)	272 (178–376)
5 Brush	1,089 (924–1,254)	323 (244–403)	471 (304–682)	277 (178–376)
6 Dormant Brush Hardwood Slash	1,089 (924–1,254)	323 (244–403)	471 (304–682)	277 (178–376)
8 Closed Timber Litter 9 Hardwood Litter 10 Timber Litter& Understory	693 (594–792)	455 (396–515)	447 (370–448)	378 (255–452)

*Based on San Dimas Technology & Development Center, Tech Tip – 1151-1805P, Fireline Production Rates, 2011. No data was collected in fuel models 3, 7, and 11–13.
**Numbers in parentheses are expected ranges of line production.
***IA = Initial Attack

We propose that for the wide area search mission for USAR, the units of measurement to be "structures per hour," and then further explore the other attributes that may be relevant. Our fundamental hypothesis is that the amount of time it takes to conduct a primary search on a building is at least partially influenced by the level of damage that structure has sustained, so we can then look at the types of damage we can expect in an area. Given the disasters that typically generate a need for wide area search are hurricanes, floods, and tornadoes, the types of damage conditions encountered would be wind damage, surge inundation damage, and floodwaters (receded or still in place). For additional cases such as earthquakes, we would also expect structural collapse. The type of work that a USAR team does can be defined by their search types: recon, hasty, primary, secondary low, secondary high, and targeted. The environment the wide area search is conducted could be rural, suburban, or urban. Lastly, a key attribute to consider would be the housing category in these areas, as that can influence how long a search of the structure takes: single family, small multi-family, large multi-family, and large commercial. Our proposed categories for future definitions of production rates would then be all of the various combinations. This proposed table of categories requires validation and refinement by the USAR practitioners.

Table 3: Proposed USAR Production Rate Categories

Housing Density	Housing Category	Conditions	Work
Rural	Single-family	Wind Damage	Recon
Suburban	Small Multi-family	Surge Damage	Hasty
Urban	Large Multi-family	Flood (receded)	Primary
	Commercial	Flood (in progress)	Secondary Low
		Shaking/Collapse	Secondary High
			Targeted

For any given production rate, the attributes would include one or more attributes from each column. For example, the rate in structures per hour of conducting a hasty search in a suburban neighborhood comprised of single-family homes after a wind damage event would be different than the rate in structures per hour of conducting a primary search in an urban area with a mix of housing types after a surge event.

Data collected by USAR does not capture the housing density, housing category, or conditions. The data collected does capture the work being conducted and the structure damage observed. Based on correlated collected data with other data sets, we determine that the production rate we could characterize would be for a primary search production of an area that was a mix of urban and suburban housing density

containing each of the housing category types, after experiencing wind damage, surge damage, and flood damage, most of which had receded. Future efforts will need to break these attributes down further to develop more granular and accurate production rate estimates.

4.1.1 Production Rate Model

Numerous attempts were made to estimate the time required to search a given structure given the damage level of that structure. These are documented in Appendix A: Exploratory Analyses. Unfortunately, the data collected by USAR teams does not necessarily reflect the timing of their operations. An ideal data collection would start a timer as a search of a structure is started, and stop the timer once the search is completed. For rescue workers operating in a lifesaving situation, where data collection is secondary or tertiary to their actions, such high-fidelity data recording is an unrealistic expectation, unless enabled by automation. As such, we had to look at batches of data recorded over a period of time by a team conducting searches. We may not be able to determine how long it takes to search a single structure, but if we have a data record at the beginning of the operational period, and a data record at the end of the operational period, we can estimate how long it takes to search that group of structures and then look at the distribution of damage within that group. Notional examples of these distributions are shown in Table 3.

Table 4: Notional Team Search Time and Damage Distributions

Team	Work Time	Damage Distribution
Team 1	5 hours	100 unaffected 50 affected 30 minor damage 10 major damage 0 destroyed
Team 2	8 hours	10 unaffected 30 affected 200 minor damage 100 major damage 5 destroyed

A Probabilistic Graph Model (PGM) was constructed to capture these distributions in the data, assuming each batch search time is the sum of each building's search time, plus travel and rest times between buildings. Using Bayesian Inference, the model can then estimate the probability of clearance times for any input batch of damage distributions.

The implementation of this model allows for an input of numerous distributions of structure counts and damage, and returns one or more rows representing probabilistic time estimates to clear the provided structure count with specified damage levels. The output times include three values: the fifth percentile representing the most likely fastest time to complete these structures, the median, representing the most common likely time to complete these structures, and the 95th percentile representing the slowest likely time to clear the provided structures. Note that this range of times from slowest to fastest with a median value is in keeping with other production rates found in industry, such as the aforementioned Wisconsin DOT road construction rates and the USFS Fireline production rates.

In the example below, the number of structures in each damage category were provided to the model:

Unaffected	Affected	Minor	Major	Destroyed
50	50	0	20	50

The model then returns the time range of 34.5 minutes to 188.6 minutes, with a median time of 91.4 minutes. The figure below visualizes all of the probabilistic distributions of time for this batch of structures.

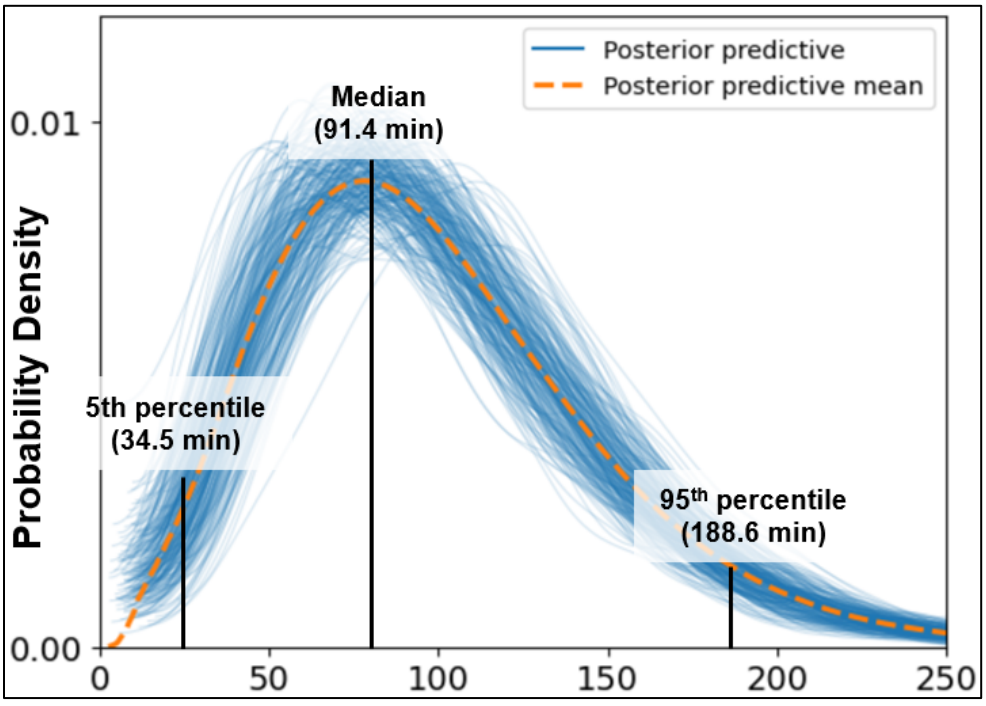

Figure 1. Probability density vs. time for estimated search time with a given damage distribution of structures.

As mentioned before, using this model in a disaster operation requires some estimation of structure damage for the disaster area as an input. Our approach to estimating that damage distribution is discussed in the next section.

4.2 FORECASTING THE CONDITIONS OF THE DISASTER

Once we have a good understanding of production rate, we could then forecast the production time required for a given disaster area. However, we know that the damage level of structures has an impact on the production rate, so we would need to be able to estimate what the damage levels would be in the area we are trying to forecast the production rate for.

A promising model has been under development by the Federal Emergency Management Agency (FEMA) for several years. Initially called the Priority Operation Support Tool (POST), it has recently grown to be a component of the Tool for Emergency Management Prioritization and Operations (TEMPO) (FEMA / New Light Technologies, n.d.). Per a FEMA fact sheet on POST: "POST's predictive model calculates levels of projected risk and exposure through a series of complex algorithms that account for hazards, the distribution and characteristics of structures and infrastructure, and population vulnerability indicators." The output of this tool is a geospatial data set of 1 kilometer of square polygons, aligned with the U.S. National Grid, enriched with data describing the area within that grid. Data includes basic demographic information on the population, number of buildings, and risk exposure metrics based on the specific damage models used.

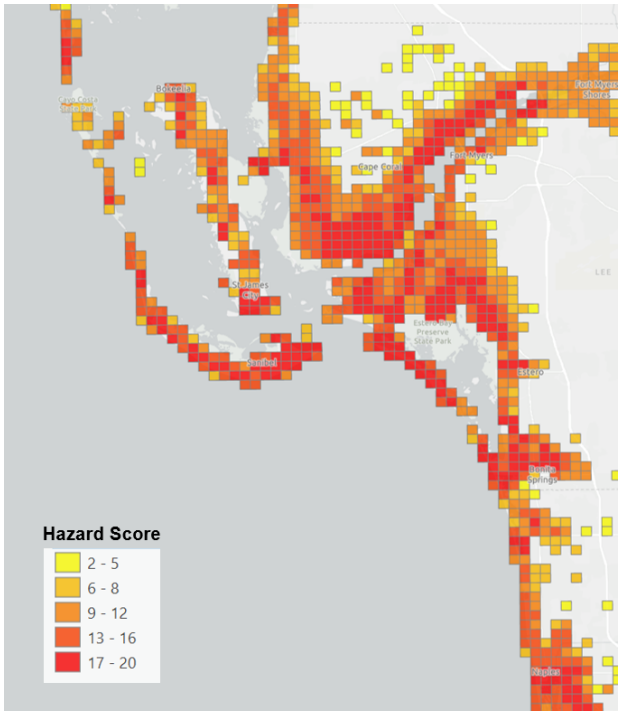

Figure 2. POST output for Hurricane Ian, showing the USNG 1km squares color coded according to their Hazard Score.

Some challenges do exist with leveraging this product as part of a system. The model and output are constantly evolving and improving, which results in differences in schemas and interpretation of the risk scores. This evolution makes it difficult to compare current iterations with past iterations, so any model that we can build would be limited to one sample and require future disasters to validate the results against.

Another challenge is that the tool may be run multiple times for an event, each time with better input data. This results in a better product as the disaster unfolds. The challenge lies in determining at what point in a disaster's lifecycle should the POST output be used as an input to estimate damage for USAR.

Lastly, as can be seen in the Figure below, the geographic area covered by POST predictions does not fully align with the geographic areas where USAR work was performed. In this example, with a few exceptions, most USAR work was done in areas covered by POST. However, not all POST grids resulted in USAR work being done. There are many possible reasons for this, among them: the damage didn't materialize as badly as predicted in that area, or the public safety resources in that area were able to support lifesaving efforts and USAR resources were not requested.

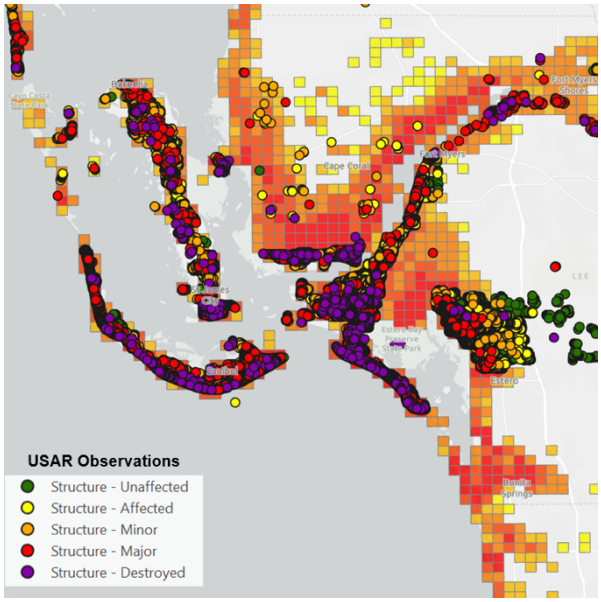

Figure 3. Overlay of USAR damage observations relative to POST output for Hurricane Ian.

Despite these challenges, given it is the most long standing and comprehensive predictive model for large disasters that generate the need for a wide area search, we decided to proceed with using POST as the way to predict damage as an input into calculating the production rate for an area. To do this, we conducted a number of analyses to determine what correlation, if any, existed between POST predicted Hazard Score and the USAR structure damage observations in that area. Details of the attempts that moved us closer to understanding that relationship can be found in Appendix A: Exploratory Analyses.

4.2.1 Damage Forecast Model

The solution that ultimately proved most viable as an input to our system concept was a Bayesian Probabilistic Graphical Model (PGM). The details of this model can be found in Appendix B: A Bayesian Probabilistic Model for Estimating Damage Distribution from Forecasts.

Functionally, the model takes as an input a set of structure counts and their corresponding Hazard Score. This allows for a distribution of structures to be submitted to the model without being restricted by the boundary of the USNG grid those structures fall in. The model then returns a series of probabilistic distributions of damage. Each row returned represents a possible outcome. For example, if the area being analyzed crossed several USNG grids with different Hazard Score values, that distribution of structures and hazard scores could be provided as input, and the model would return several possible distributions of damage. The damage scale used is the same as the USAR observations: unaffected, affected, minor, major, and destroyed.

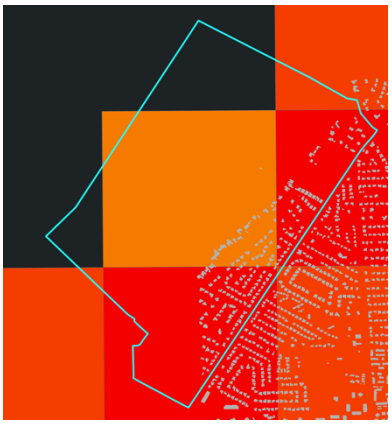

Hazard Score	Building Count
11	44
16	1
17	98
18	62
Bldg. Count	205

destroyed	major	minor	affected	unaffected
49	38	32	55	31
40	64	32	45	24
39	18	23	21	104
19	7	69	107	3
0	45	79	49	32
2	58	31	30	84
0	99	63	21	22
37	65	25	77	1
104	0	11	38	52
71	34	69	7	24

Figure 4. Left: A polygon highlights buildings spread across several USNG grids with different Hazard Scores. Middle: The number of buildings in each grid are tabulated and provided as input to the model. Right: 10 possible outcomes of damage.

Using this model in a disaster operation would require the input of search segment polygons in order to tabulate the structures and corresponding hazard scores. Our goal in generating those search segments is described in the next section.

4.3 EQUALLY SEGMENTING AN AREA

A key tenet of wide area search is breaking the area into subsections to be searched. This "segmentation" facilitates distributing the search effort across multiple teams and enables tracking of progress. For events that cover a large geographic area, segmentation can become a significant challenge.

The methodologies involved in search segmentation aim to keep segments at manageable sizes and follow some rules that support ease of movement of USAR teams in that segment. For example, segments may be bounded by naturally occurring boundaries such as rivers, or by barriers in the built environment such as highways.

Under the intense time sensitive conditions of a large geographic disaster, externally defined boundaries have been used as predetermined segments, with varying results:

- US National Grid: This 1km grid is an externally defined boundary set that does segment an area into equal areas. However, there is no guarantee that the boundaries created will align with the damaged area, encompass the built environment to be searched, or contain equal numbers of roads and structures to be searched.

- Postal Zip Code: This pre-existing boundary presents a lot of the same challenges as USNG, but also consists of widely varying geographic scales and thus population density; A zip code in Tonopah, NV encompasses 10,000 square miles, while a zip code in Manhattan covers two city blocks (National Public Radio, 2013).

- US Census Boundaries: The US Census provides boundaries that are based on population, topography, and housing characteristics. The boundaries are also based on "nonvisible boundaries, such as selected property lines and city, township, school district, and county limits" (US Census Bureau, n.d.). These invisible lines inject boundaries that can make Census geographies an inefficient means of segmenting an area and violate the goals of wide area segmentation. In some locations, this is not an issue, and in other locations it can create segments that are nonsensical for search planning. The three major geographic Census boundaries considered are:

    - Census Tract: The Tract level of Census can be inconsistent in geographic size. The Census Tract is often too large, geographically, for a search segment.

    - Census Block: This is the smallest geographic Census area, but is often too small to be a worthwhile segment.

    - Census Block Group: This boundary is a collection of blocks, clustered based on their numerical identification.

Our goal, then, is to use the extent of disaster damage to bound a populated area and then subdivide that area into segments that conform to the tenets of wide area search and result in areas of roughly equal work. Operationally, we see this initial segmentation as just that—an initial cut at the problem that gives the USAR search planning experts a starting place and supporting data to refine the segmentation.

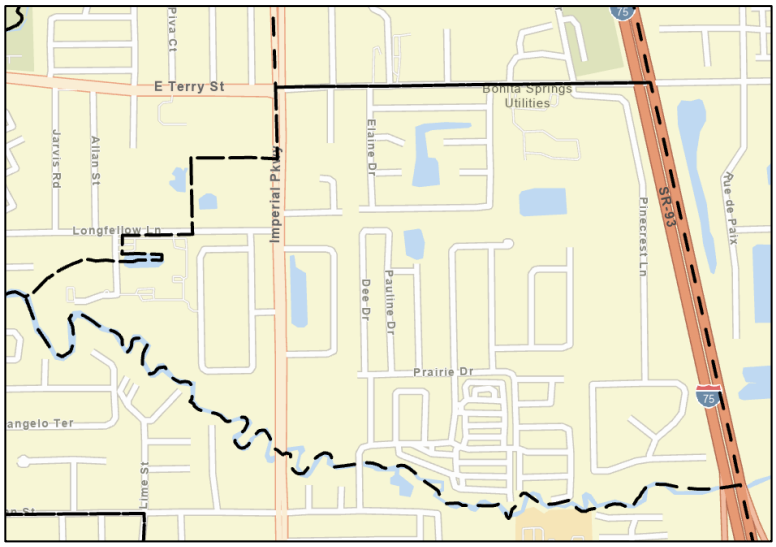

Figure 5. Census Block Group in Ft. Meyers, FL. There is no way to access all of the roads within the boundary without traveling outside of the boundary.

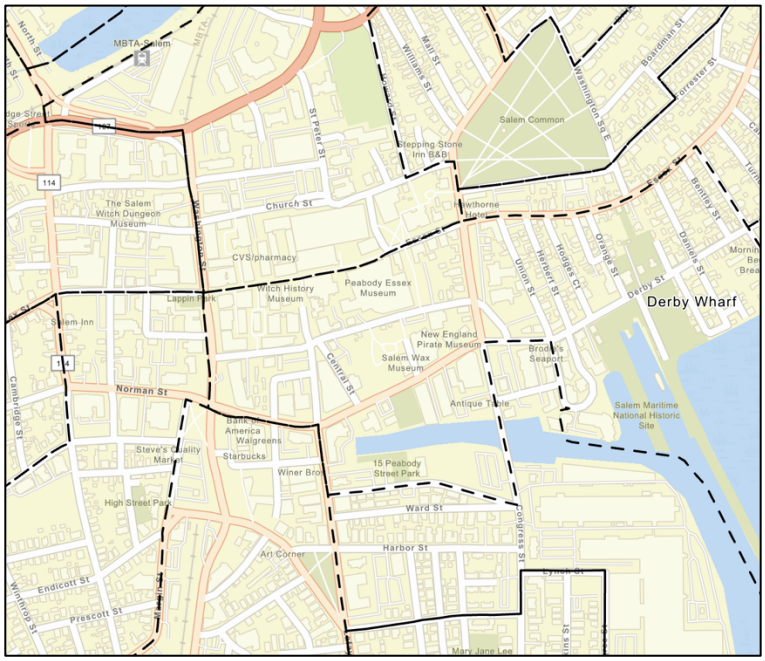

Figure 6. Census Block Groups for Salem, MA. Boundaries would have USAR teams crossing major roadways or water canals, or backtrack significantly to cover all roads.

4.3.1 City Partitioning Algorithm

Numerous approaches to this problem were explored, and are described in more detail in Appendix A: Exploratory Analyses. The final demonstration algorithm implemented an approach that combined "half-splitting" and iteration cleanup. Technical details on the algorithm can be found in Appendix C: City Partitioning to Enable Balanced Emergency Response Efforts.

The algorithm was tested against a section of Tampa, FL which contains several features that could present a challenge to the algorithm, such as neighborhoods with low connectivity to surrounding areas, waterways, and major highways. Shown in Figure 5, each partition conforms to the rules provided and resulted in the number of buildings being 15 percent of optimal or better.

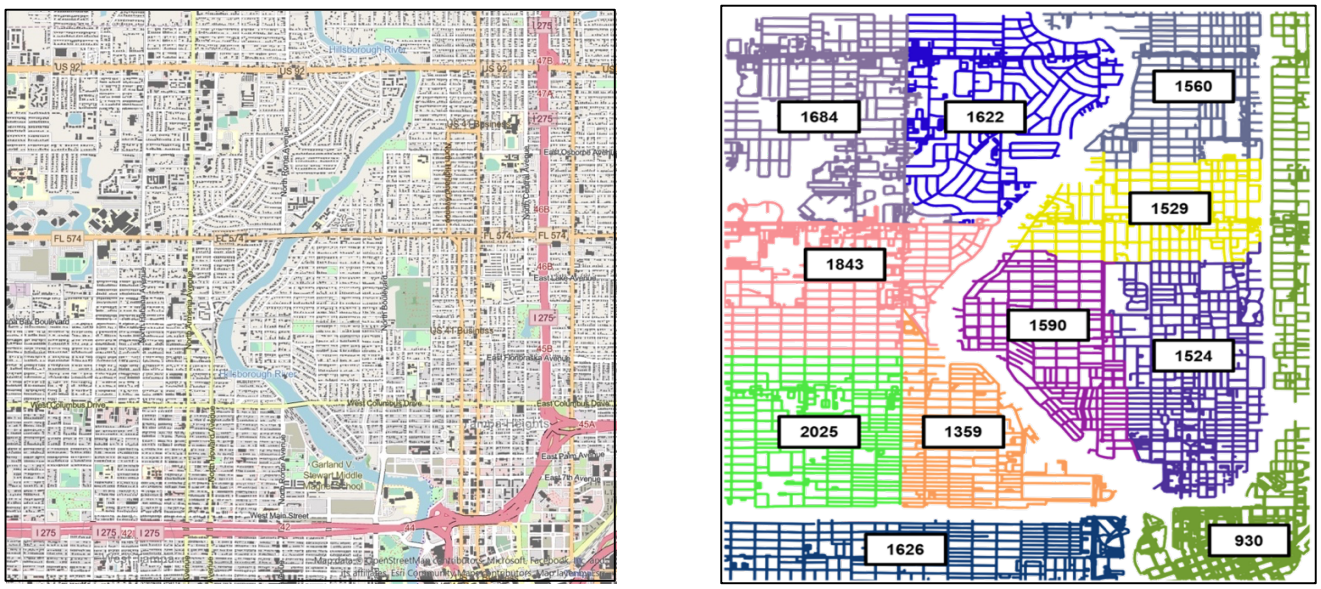

Figure 7. Left: Map of Tampa, FL from OpenStreetMap showing building footprints. Right: Partitioning output showing the number of structures for each color coded partition.

Future Work: At the conclusion of this effort, the partitioning algorithm uses the number of buildings as the metric for determining equal segments. In order to provide the most value in a disaster planning scenario, this metric needs to be expanded to represent equal amounts of work, as determined by the Damage Forecast and Production Rate models. Further benefit and predictive accuracy for work requirements would augment both models with structure specific details such as housing type.

5. PIPELINE PROTOTYPE

The individual components to this system are intended to work together to provide the end user with an initial set of well informed and intelligently created search segments, an estimate of the damage they expect to find, and the amount of time that clearing an area will take. The complexity and implementation time of the partitioning algorithm meant that a demonstration pipeline would initially require some external set of boundaries. Despite the challenges described in Section 5.3, we opted to use Census Block Groups for the demonstration pipeline to capture some performance metrics and visualizations of what the ultimate output of this system could be.

For this pipeline, the inputs are:

1. POST Damage Forecast in shapefile format
2. Building footprint polygons as a shapefile for the general area of interest
3. A set of polygons in shapefile format that represent smaller geographic areas that can be used as search segments; in this case, Census Block Groups

The outputs generated are:

1. Polygons representing each area of interest that falls within a county boundary and hugs close to the outer edges of the POST input data
2. Building footprints enriched with the POST Hazard Score for the grid the building is in
3. A shapefile containing the polygons provided as input search segments, enriched with the following attributes:
    a. Estimated number of buildings that would be Unaffected
    b. Estimated number of buildings that would be Affected
    c. Estimated number of buildings that would have Minor damage
    d. Estimated number of buildings that would have Major damage
    e. Estimated number of buildings that would be Destroyed
    f. The fastest likely time it would take to conduct a primary search of all of the buildings in the segment
    g. The median likely time it would take to conduct a primary search of all of the buildings in the segment
    h. The slowest likely time it would take to conduct a primary search of all of the buildings in the segment

5.1 PREPROCESSING

The first step in the pipeline performs some preprocessing, taking the POST damage forecast and relevant building footprints to produce smaller Area of Interest (AOI) polygons and enrich the building footprints with the POST hazard score.

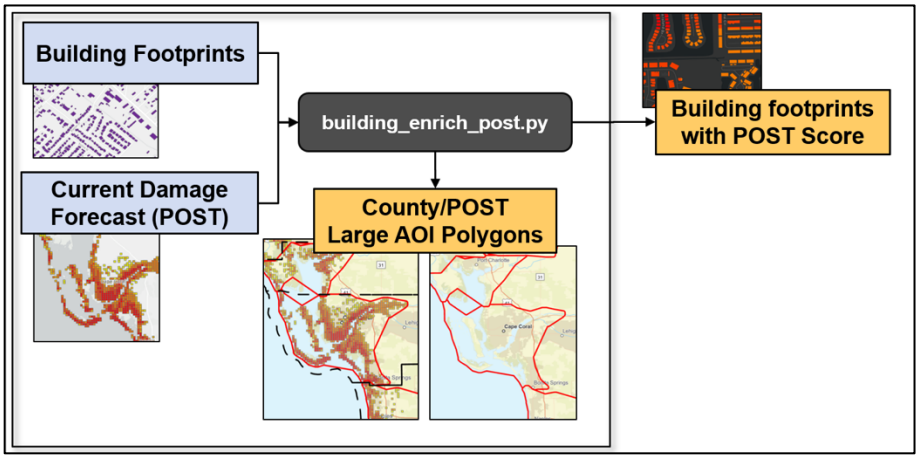

Figure 8. Preprocessing in demonstration pipeline.

The county constrained AOI that outlines the POST damage estimates serves as a way to subsection the POST data within the County administrative boundaries which are very often used to divide wide area searches into branches or divisions.

5.2 ESTIMATED DAMAGE DISTRIBUTION

The next step in the pipeline is to estimate the damage distribution across the structures within each segment, based on the building's POST hazard score. This involves iterating through each search segment and tabulating the building count per POST hazard score, and passing that distribution to the Damage Forecast Model. That model returns one or more potential probabilistic damage distributions.

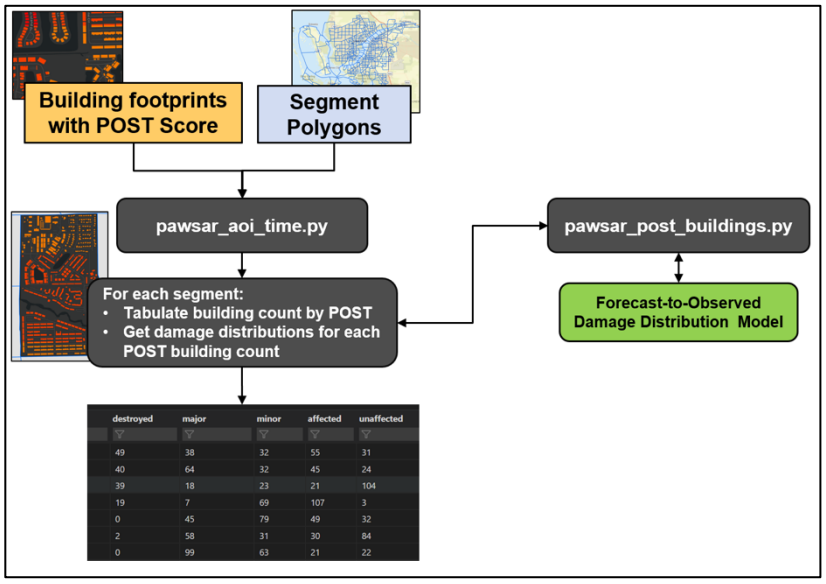

Figure 9. Estimated damage distribution in demonstration pipeline.

The output from the Damage Forecast Model is stored in memory and passed along as an input to the Production Rate model and the structure damage distribution counts are added as attributes to the current segment polygon.

5.3 PRODUCTION RATE: DAMAGE DISTRIBUTION TO CLEARANCE TIME

This portion of the pipeline passes the distribution of structures with corresponding estimated damage levels to the Damage Distribution to Clearance Time Model. The result of this is a distribution of clearance time ranges, indicating the fastest, median, and slowest likely times required to conduct a primary search of the structures with the provided damage distributions. These values are then added as attributes to the current segment polygon.

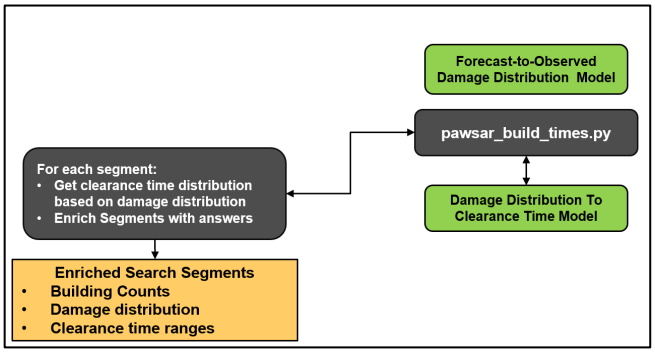

Figure 10. Production rate estimation in demonstration pipeline.

After this step is finished, the pipeline iterates to the next search segment until done. The final output is a shapefile containing the search segment polygons enriched with the attributes indicating building damage distributions and estimated clearance times.

5.4 SAMPLE OUTPUT

A sample visualization of the final product is below, where each search segment is color coded according to the median expected time to conduct a search.

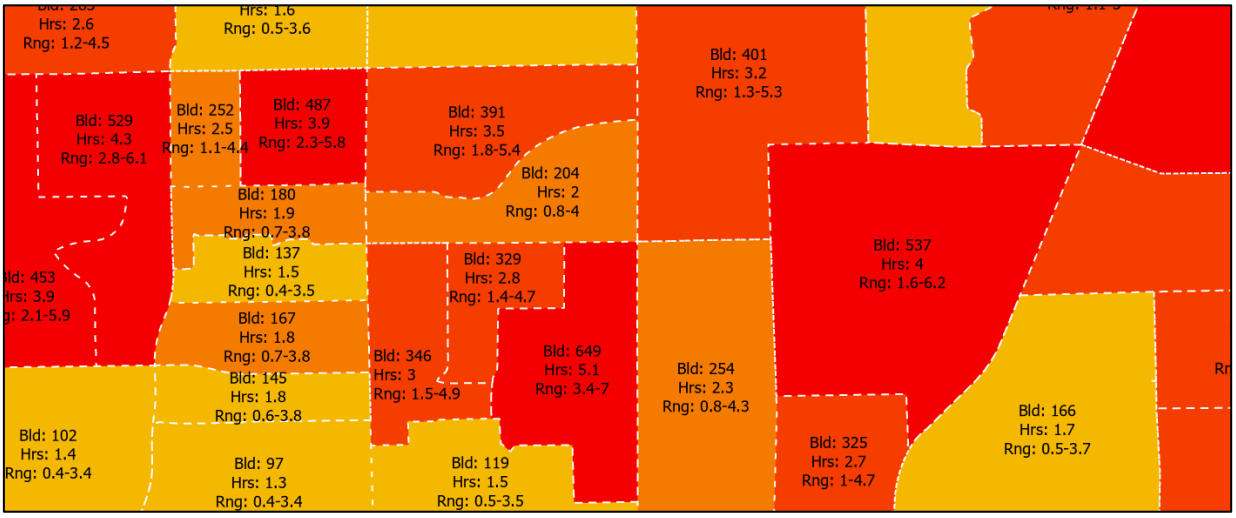

Figure 11. Sample output showing building count and estimate clearance times for search segments. Color coding represents fastest (yellow) to slowest (red).

FID	Shape	e_unaff	e_aff	e_min	e_maj	e_dest	e_bldcnt	et_025	et_5	et_975
0	Polygon	55	250	84	101	39	529	158	262	377
1	Polygon	182	36	16	12	37	283	68	151	266
2	Polygon	224	0	18	3	9	254	50	136	254
3	Polygon	393	2	0	4	2	401	76	191	314
4	Polygon	11	0	0	4	82	97	21	81	204
5	Polygon	45	44	14	45	2	150	35	102	221
6	Polygon	53	3	16	304	15	391	114	202	315
7	Polygon	10	27	71	48	11	167	40	107	225
8	Polygon	29	0	10	103	3	145	34	100	219
9	Polygon	39	10	188	3	5	245	56	130	245

Figure 12. Sample data view of enriched polygons.

The output is produced in shapefile format.

5.5 PIPELINE PERFORMANCE

To evaluate the viability of this concept to the urgent environment of a wide area search, we conducted some time trials of pipeline operations using a standard laptop computer. The estimated time required for each of the major pipeline steps are as follows:

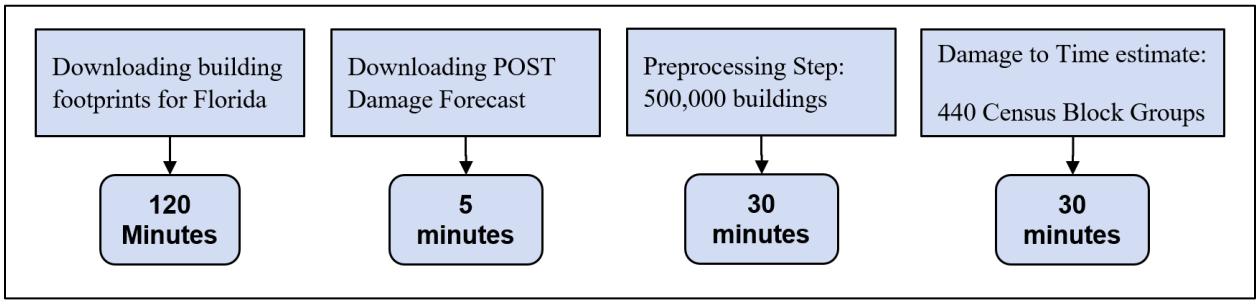

Figure 13. Pipeline performance estimate.

The initial downloading of data is a one-time effort and in the case of a hurricane response could be done as a preparatory step well before USAR team deployments.

From there, the combined time from a new POST output to a new set of search segments is about 65 minutes. From an operational standpoint in the hurricane context, if a new POST model were to come out once per operational period, up until hurricane landfall, a set of enriched search segments could be available to be used to support the USAR planning cycle within about one hour.

This pipeline has not undergone any performance optimizations and could likely be improved.

This page intentionally left blank.

6. DISCUSSION AND RECCOMENDATIONS

In this section, we present some observations and recommendations based on the research and analysis conducted over the lifespan of this project.

6.1 OPERATIONAL INSIGHTS

With exploratory data analysis, we were able to identify some aspect of USAR operations that may be of immediate value to those managing large scale wide area searches. In some cases, these observations are self-evident (such as a secondary search takes longer to complete than a primary search), but the fact that the data analysis confirms this reinforces the validity of the analysis. The insights are broken out temporally, as a response unfolds over time.

Day 1

- Recon takes longer than it does on later days.
- The total area searched by a squad varies more than on other days.
- Total area covered by a squad area averages 9 mi^2, including travel from Base of Operation and recon activities.
- Searches tend to start in the center of the urban area affected by the disaster.
- Searches conducted on this day are faster than searches later in the response and are typically of type recon and hasty.

Middle of the Response

- Recon searches are faster than on Day 1.
- Areas searched by squads overlap each other, potentially indicating duplication of effort.
- Areas searched average 1.75 mi^2 per squad.
- Secondary searches start to take place in some areas.
- Secondary searches take longer than the other search types.

Last Day

- Recon is fastest.

- The final day has a greater distance between searches.
- The total area searched by a squad varies more than on previous days.
- Searches generally take less time.

6.2 TESTING AND VALIDATION

The three predictive tools developed (1. production rate estimation, 2. forecast to observed damage correlation, and 3. automatic city partitioning) were done primarily with data from Hurricane Ian. The work demonstrates that the data collected by USAR teams can be used to establish predictive models and inform intelligent partitioning, but more work is needed to determine how well these predictive models perform. Original project plans included running the models against a new hurricane to being to collect data on the accuracy of the models, however there were no significant hurricane landfalls that required large wide area search efforts from USAR during the summer/early fall of 2023.

6.3 PRODUCTION RATE DEFINITIONS

Central to the concepts presented to this work is standardization of how USAR work is quantified. It is recommended that the USAR community begin to consider the Production Rate attributes presented in section 5.1: Establish Production Rate Estimates for Different Conditions. As with other production rate standards, the establishment of these attributes would be best done as a collaboration between USAR experts and data science experts. It is important to note that the establishment of metrics should not be used as a way to elevate some teams or disparage others, but rather as a way to understand the current baseline and how all teams can then incrementally cross share methods and training. It is also entirely possible, even likely, that USAR teams are already performing at the highest level possible, but without metrics it is impossible to know for certain.

6.4 SEARCH SEGMENTS

It is recommended that USAR continues efforts to incorporate search segmentation into the existing electronic data workflows. Breaking down a large area into smaller areas to search is foundational to wide area search methodology. Analysis of the data for Hurricanes Delta, Laura, and Ida indicate that activity at the squad level is not always bound to unique areas, resulting in overlap, duplication, and backtracking. While not the focus of this work, we did come to understand that much of the segmentation work is done at a higher geographic level and by way of marking paper maps, making it difficult for these assignments to propagate to the squad level. As of this writing, the SARCOP tool does now support electronic generation of search segments which could be pushed to squad smart devices, so that they have an in-field reference of where they are versus their assigned area. The existing tools rely on either hand-drawn segment, which are time consuming and may not be intuitive to users conducting the segmentation work, or predefined administrative boundaries such as Census Block Groups, which have pitfalls previously described.

Until such time as intelligently auto-generated search segments are available as part of the USAR planning cycle, many benefits would come from exploring ways to transition from human generated segments on paper maps to electronically available segments. While not technically advanced, a simple approach of hand-digitizing segments drawn on a paper map, assuming there is staff with the skills and time to do so, may be a reasonable stop gap.

This page intentionally left blank.

7. CONCLUSION

In this report we describe an effort to develop predictive analytics that can leverage data collected by USAR teams responding to past wide area searches and provide decision support inputs for future wide area searches. We demonstrated that it is possible to develop models to predict the expected damage in an area, how long it is likely to take to search that area, and how to segment that area into equal subparts to facilitate organized and distributed search assignments. We further demonstrated how a pipeline could be built to support integrating these models into an operational environment.

These models were developed on data collected by an evolving system that does not always represent USAR actions in high fidelity, but there is clear indication that increasingly better data collection technology, broader training, and more exercises are resulting in data sets that can represent a USAR response in great detail.

The work and recommendations described in this report can serve as a framework for building a future system that captures data for every event, incorporates that data into better models, and provides increasingly accurate predictive inputs to decisions, ultimately enabling efficient wide area searches that adapt to real time observations.

This page intentionally left blank.

APPENDIX A: EXPLORATORY ANALYSES

7.1 CONVEX HULL ANALYSIS

The convex hull of a set of points is defines as the smallest convex polygon that encloses all of the points. A convex hull polygon was created to encompass each of the points in the data for each day. This allows for visualizing the broadest geographic area encompassed by the search teams on each day of the response.

The graphics in Figure 14 show the convex hulls for structural damage data collected by USAR during the response to Hurricane Delta in 2020. Each polygon is the convex hull for one squad or sub-squad that was collecting data. Each day is assigned a unique color. Visualizing the geographic extent of data collected can show areas where there is overlap, which may be the result of duplication of effort. Day 284 shows relatively little overlap and the areas are relatively compact. Days 285 and 286 have more overlapping areas, and Day 287 has larger geographic areas that also include a lot of overlap.

The convex hull graphics for Hurricane Laura are shown in Figure 15. Each day shows more overlapping polygons indicating potential duplication of effort or other inefficiencies.

When visualizing each of these data sets cumulatively, allowing each day's convex hulls to be displayed on the same graph, it becomes clear that not only is there overlap for each day, but also overlap across all of the days. This may indicate areas being searched repeatedly. It cannot be determined from the data itself what the driver of this overlap is; it could be inefficient resource allocation, searching areas again as new information becomes available over time, or activity conducted at the direction of the Authority Having Jurisdiction.

The visualization of these two data sets does indicate that there is a lot of overlapping coverage by USAR teams. Segmenting the impact area into well-defined partitions and assigning resources to those segments could reduce the duplication and overlap.

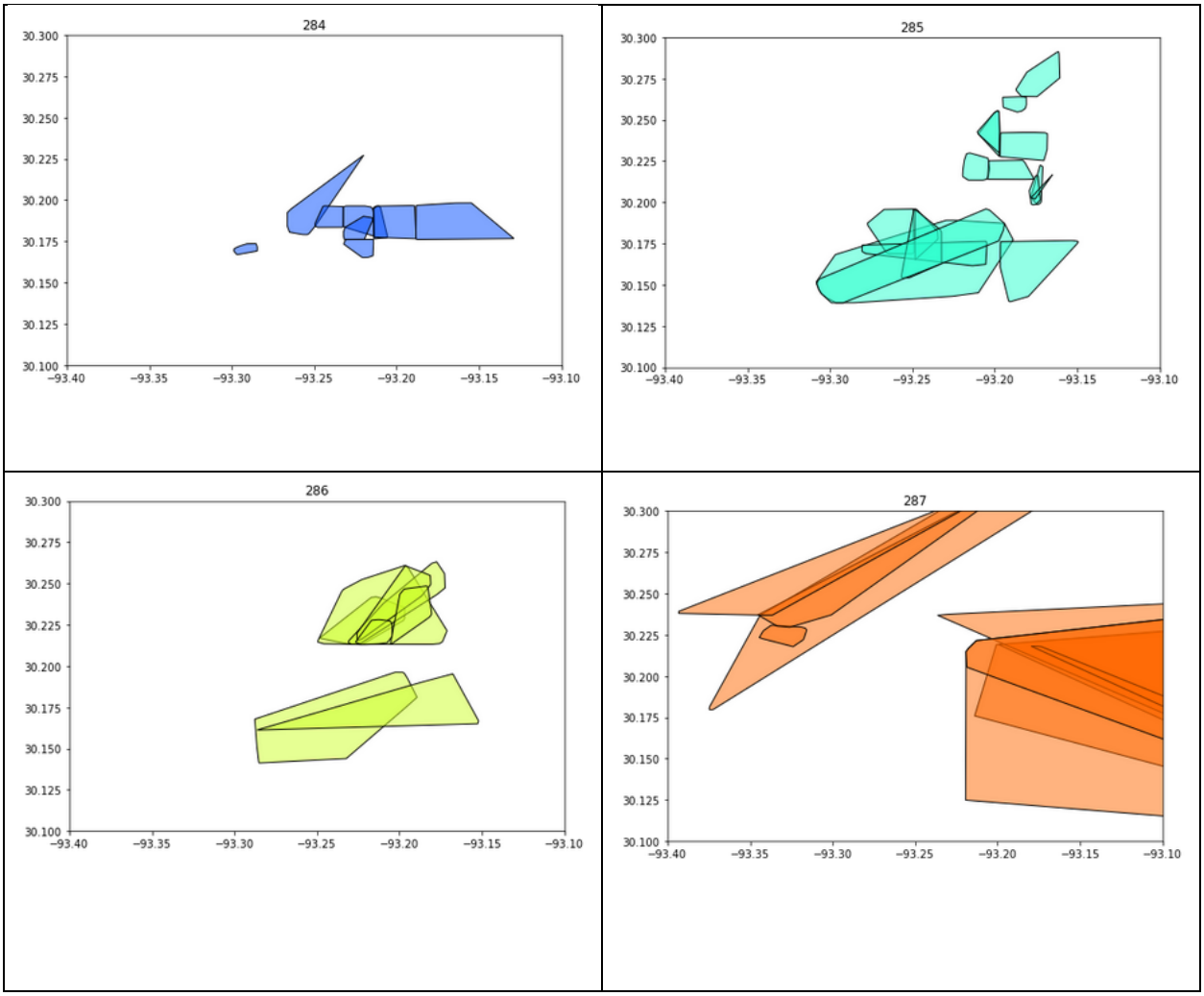

Figure 14. Hurricane Delta Daily Convex Hulls.

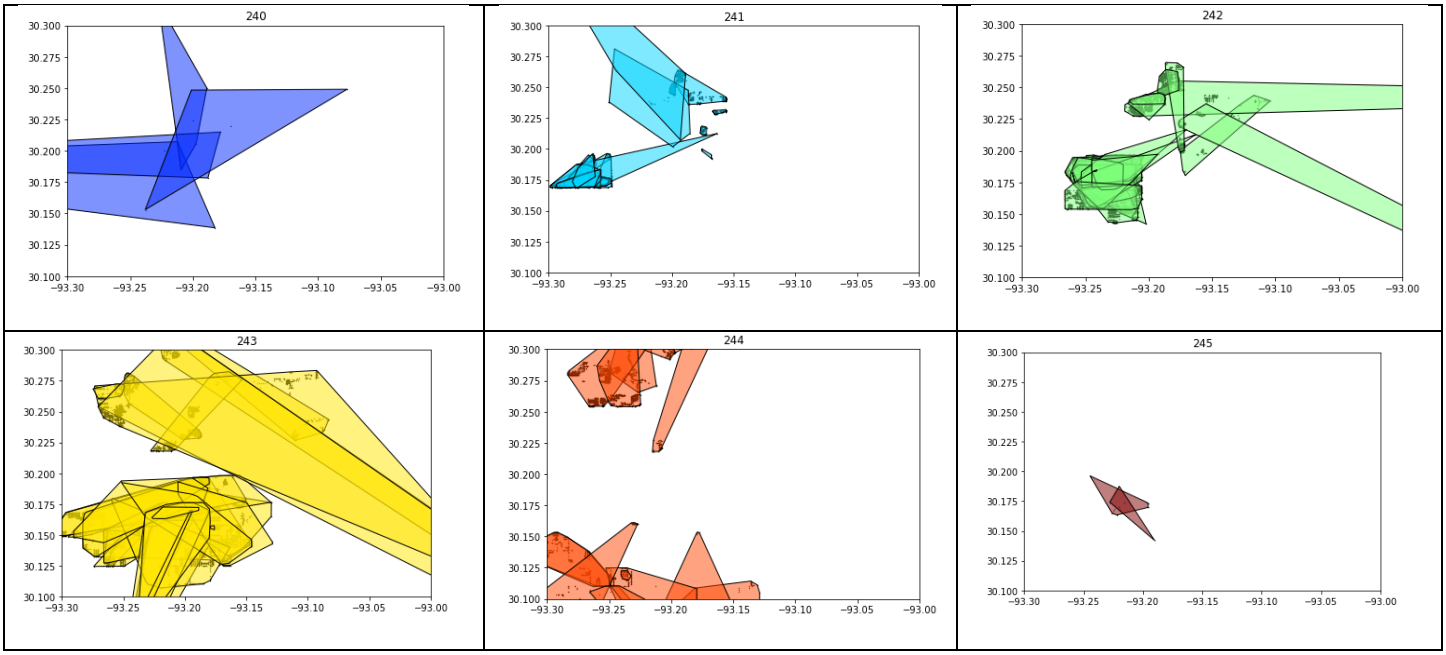

Figure 15. Hurricane Laura Daily Convex Hulls.

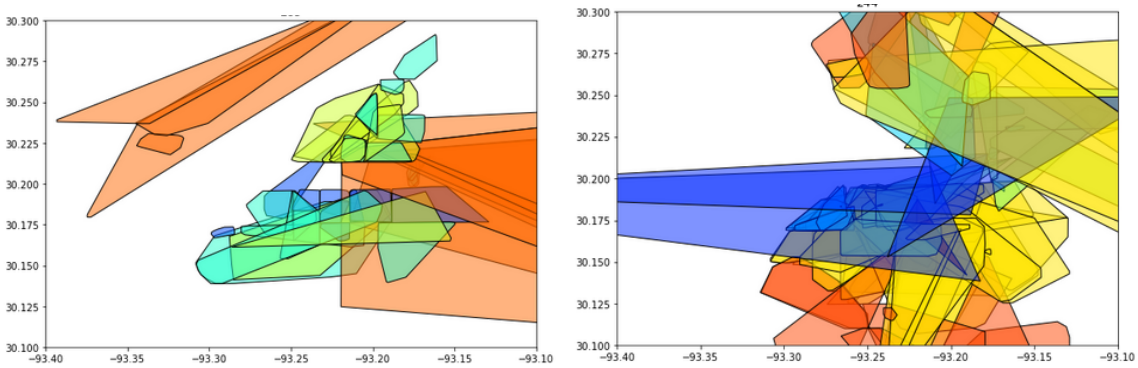

Figure 16. Hurricane Delta Cumulative Convex Hulls and Hurricane Laura Cumulative Convex Hulls.

7.2 SEARCH OCCURENCES AND DURATIONS

Plotting search times over the course of a response, separated by search type shows that searches earlier in the response tend to be shorter and searches in the middle of the response are longer.

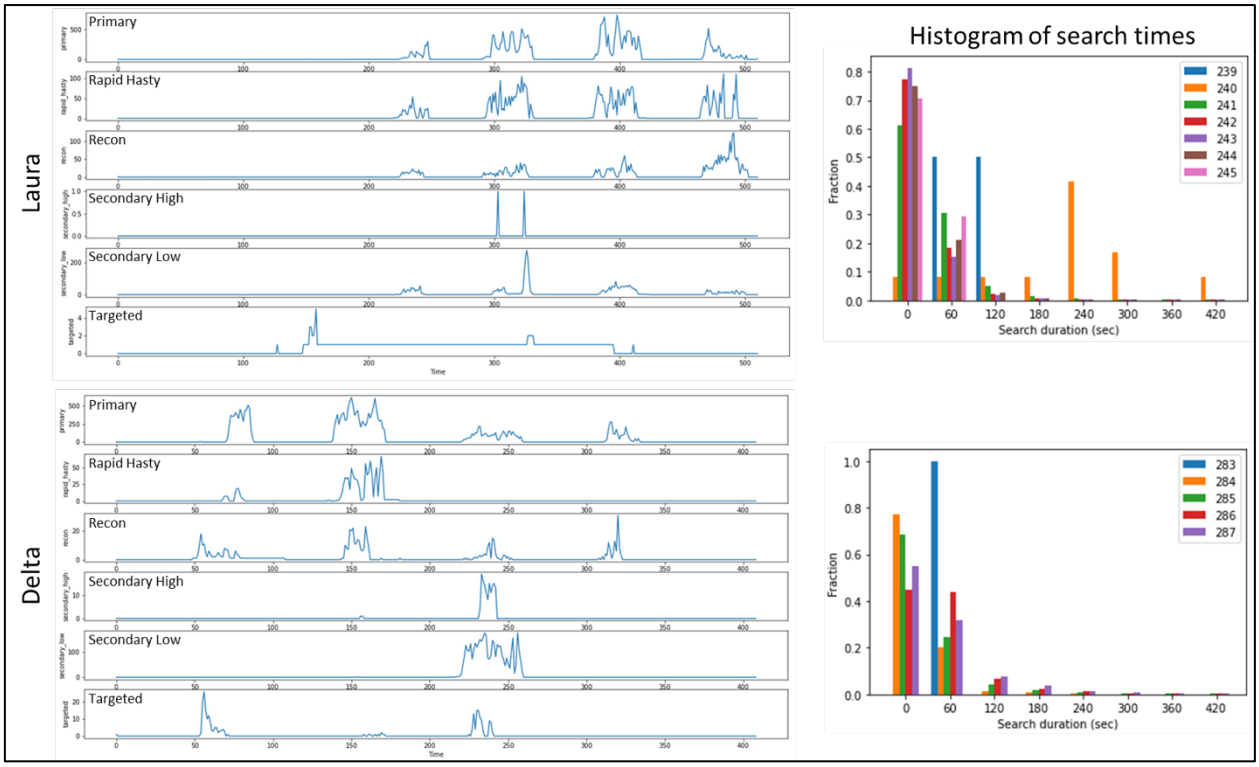

Figure 17. Histograms of search times over the course of a response.

7.3 SEARCH DURATION BY TYPE

Plotting the search times by search type for hurricanes Laura and Delta show that secondary searches tend to take longer, recon searches get faster as the response progresses, and secondary searches happen in the middle of the response.

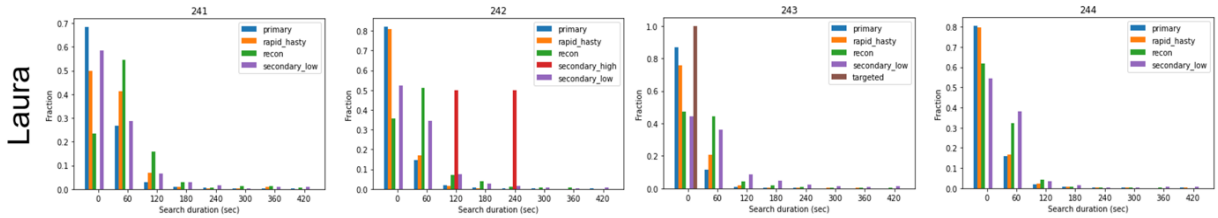

Figure 18. Search duration by type for Hurricane Laura. Histogram 241 is day one in the response.

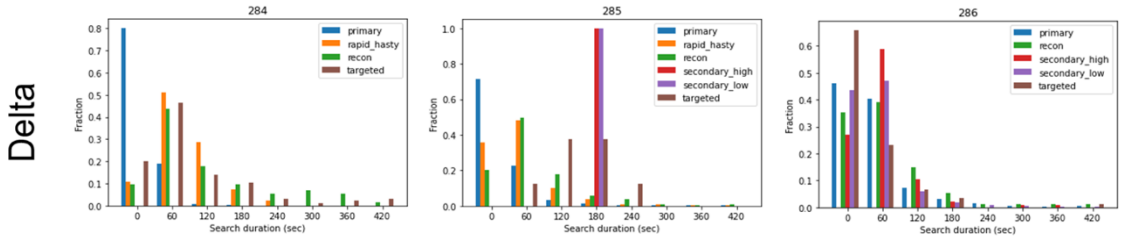

Figure 19. Search duration by type for Hurricane Delta. Histogram 284 is day one in the response.

7.4 STRUCTURES AND DISTANCES

Several visualizations of path lengths versus search counts and number of structures searched reveals several trends, consistent in both Hurricane Delta and Hurricane Laura:

- There is some correlation between the total path length (sum of linear distance covered by a squad) and the number of searched structures.
- Teammates don't add linearly—the average path shows little correlation.
- Final search day has greater distance between searches, driven by both fewer searches and longer travel distances.
- Strong correlation between individual travel distance and number of searched structures.
- Path length and number of searches have "long tails," which may indicate a high topological dependence (the layout of structures in an area).

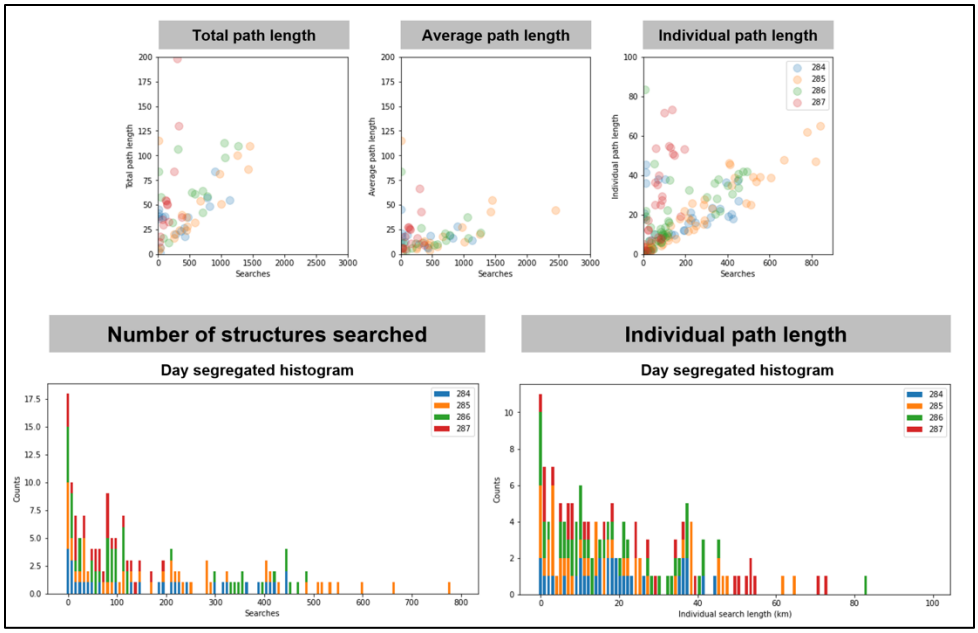

Figure 20. Hurricane Delta visualizations of search path lengths and structures searched.

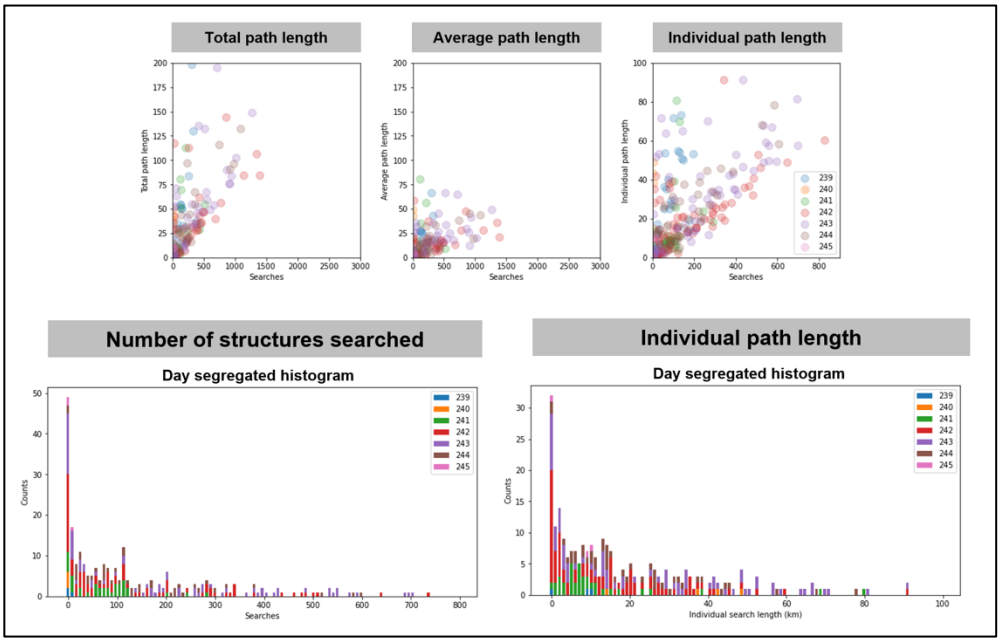

Figure 21. Hurricane Laura visualizations of search path lengths and structures searched.

7.5 AREA COVERED BY SQUAD PER DAY

Calculating the geographic area covered by each squad, each day for Hurricane Delta indicates that most squads cover the same area per day, with the most variability in area occurring on the first and last days.

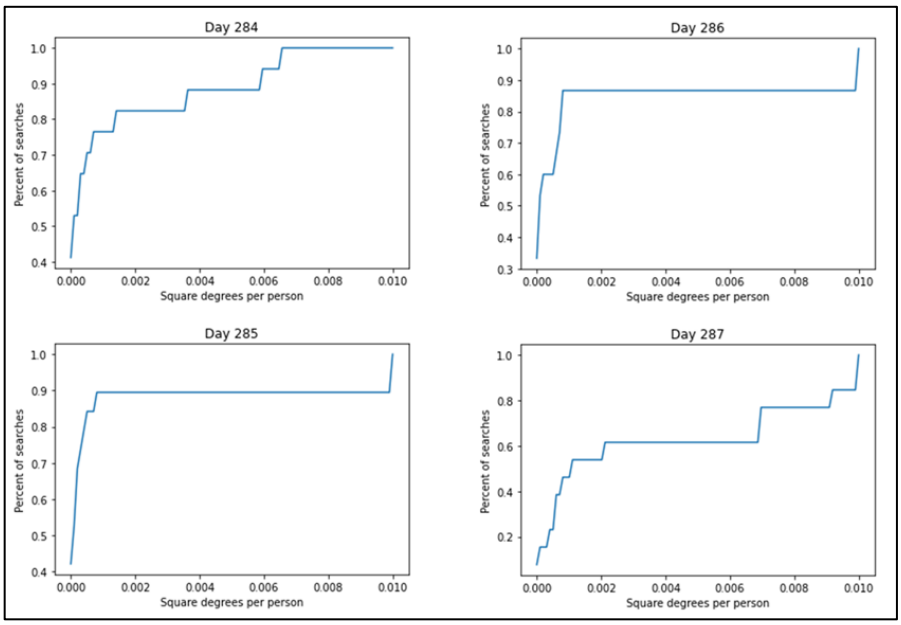

Figure 22. Area covered per squad per day for hurricane Delta.

When excluding the travel from Base of Operation to the search area, and searches of type recon, the average area covered by a squad in a day is 1.75 square miles.

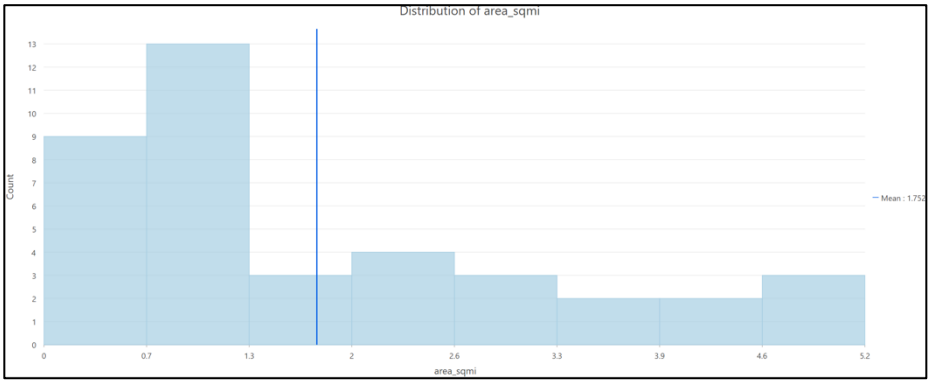

Figure 23. Area per squad excluding recon and travel.

7.6 POST / TEMPO CORRELATIONS TO OBSERVED DAMAGE

An example of analysis conducted that indicated there was some relationship between the POST Hazard Score and the level of damage observed by USAR teams. The relationship is not simple or linear, but did provide enough validation to pursue the other methods of predicting the damage distributions based on Hazard Score.

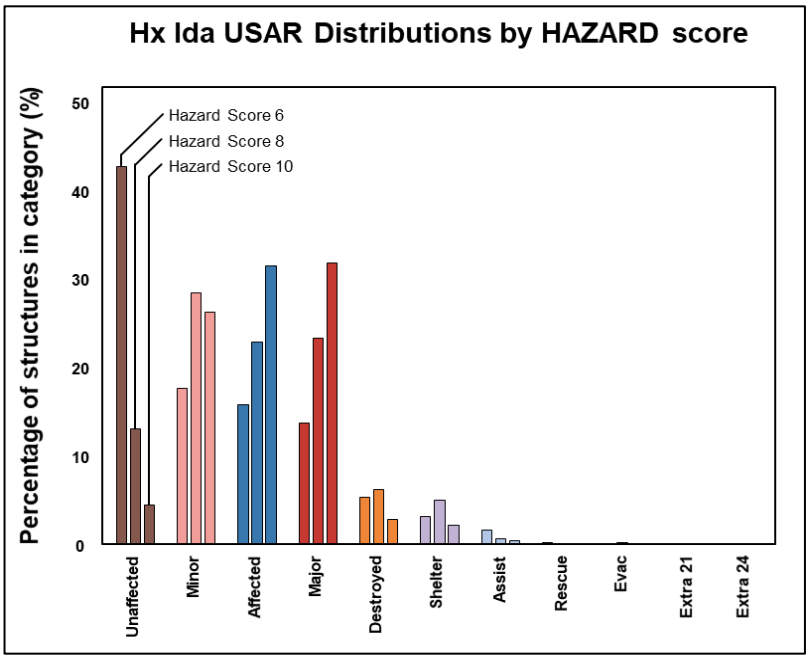

Figure 24. Percentage of structures in each damage category, clustered by POST Hazard Score.

7.7 REGRESSION MODEL APPROACH: SEARCH TIME AND DAMAGE PREDICTION

An effort was made to build a regression model for both the Hazard Score from POST as a predictor of damage and the USAR search data as a predictor of search times. Ultimately, this model did not perform well, as the relationships are not linear. The summary of this effort is presented here.

The data used for this effort was Hurricane Ida. Note: the POST hazard score is at a different scale than other references to POST data from Hurricane Ian.

Hazard Ranking vs. Waypoint Type

Because the ultimate goal of the program is to provide predictive capability, a relationship needed to be established between data available pre-disaster and data available post-disaster. In this case, Hazard ranking was used as a predictive measure of the type of damage observed. By binning the observed waypoints into their respective 1 km grids aligning with the Hazard score grid, a “damage profile” could be established at each hazard rank that captures the prevalence of each type of damage.

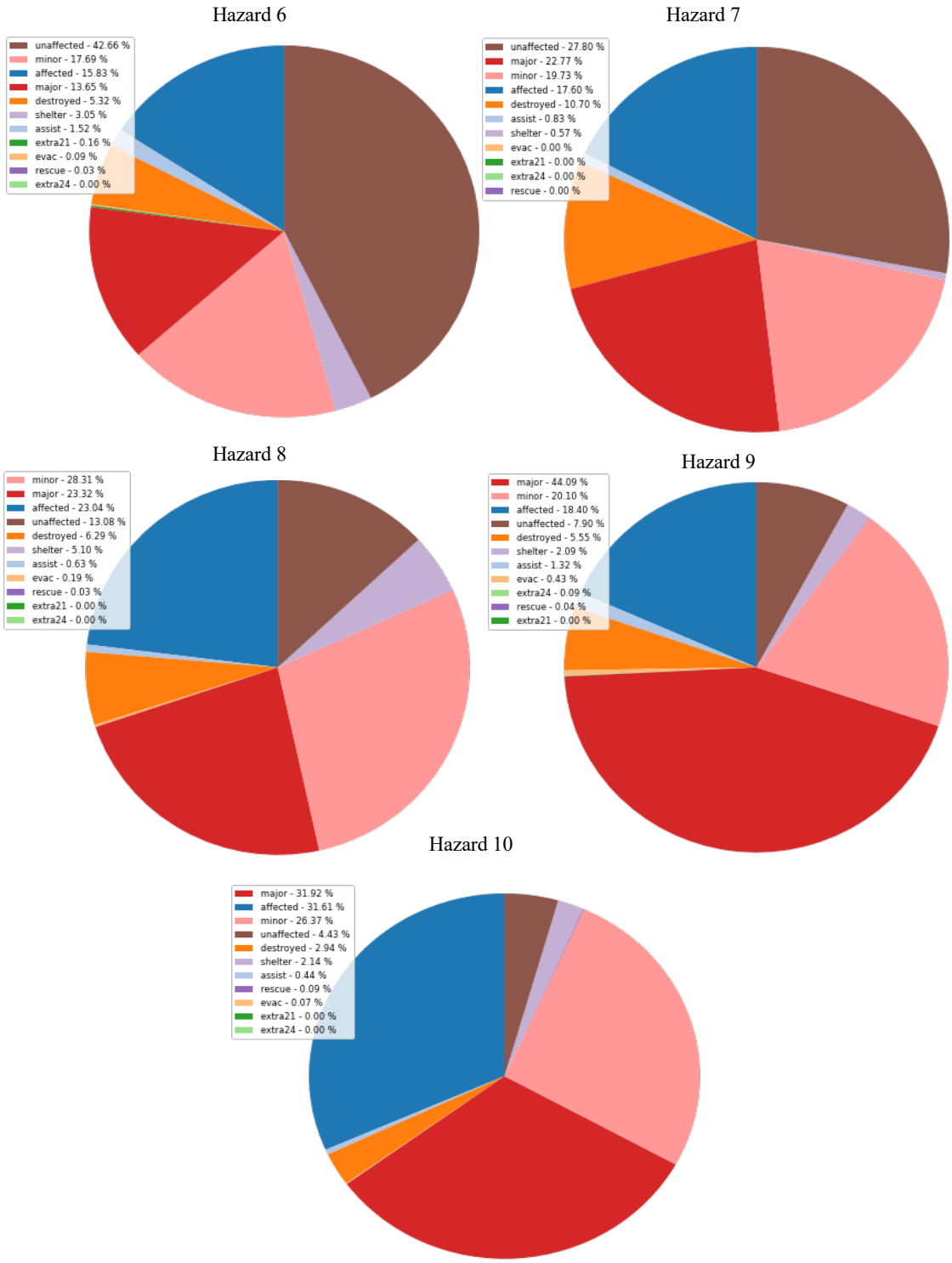

Figure 25. Distribution of Waypoint Damage by Hazard Rank for Hurricane Ida Response.

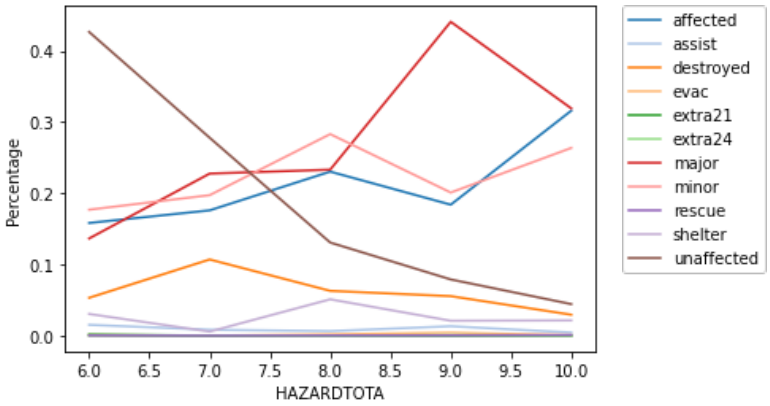

Figure 26. Percentage of Waypoint Damage Types as a function of Hazard rank.

Generally, as Hazard rank increases, the prevalence of unaffected structures decreases from 43 percent down to under 4 percent. Conversely, affected, minor, and major damaged structures increase in accordance with Hazard rank. Collectively they make up 47 percent of waypoint observations at Hazard Rank 6 and 89 percent of observations at Hazard Rank 10. This data serves as evidence that Hazard Rank is potentially predictive of resulting damage.

Search Time Distribution by Waypoint Category

In conjunction with the waypoint type distribution, it is important to characterize the expected search duration for each waypoint type to be able to produce search time estimates. To do so, cumulative distribution functions were produced for the search durations of each category of waypoint.

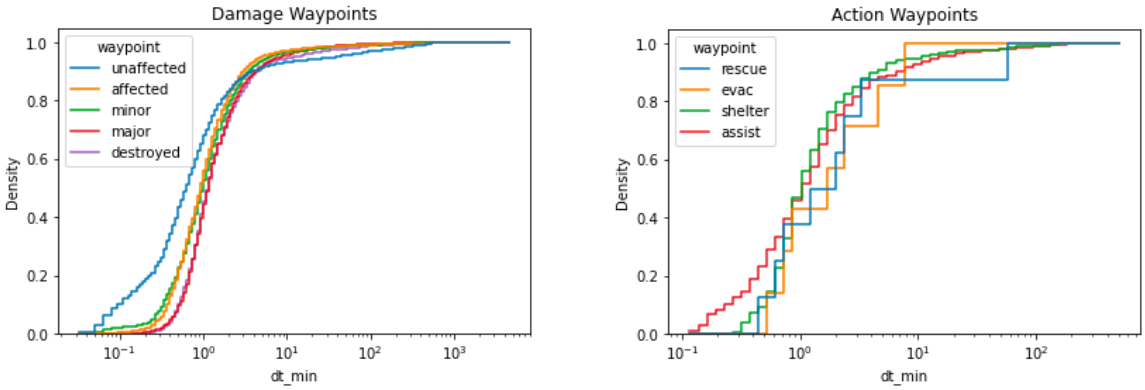

Figure 27. Cumulative distribution function of waypoint search durations (in minutes) by category.

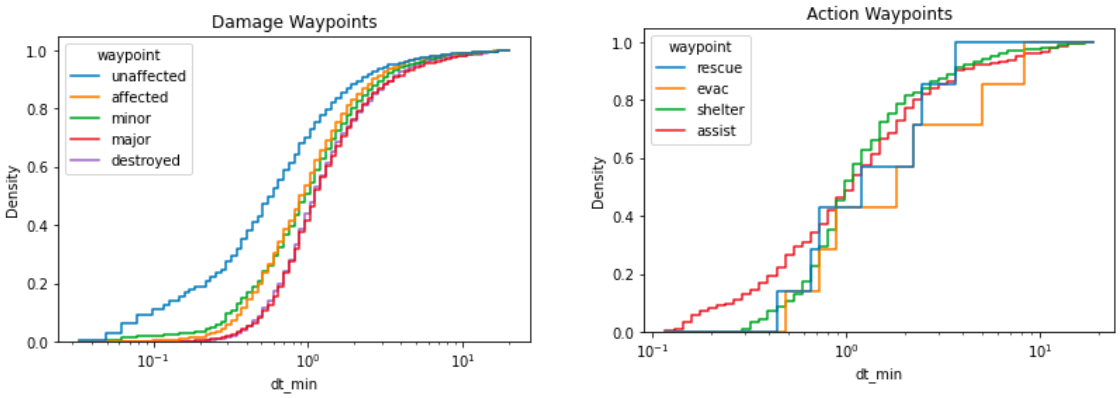

Figure 28. Cumulative distribution function of waypoint search durations (in minutes) below 20 min. by category.

There are a few takeaways from these distributions. First, unaffected waypoints appear to consistently take less time to search than other "damage" waypoints. This trend, however, is reversed for waypoints taking longer than ten minutes to search. In this upper range, the unaffected distribution has a heavier tail. Affected and minor waypoints share distributions and consistently take longer to search than unaffected waypoints. Similarly, major and destroyed waypoints share similar distributions as well and take the most time to assess among the "damage" waypoint types. These observations should be tempered by the fact that most of these search durations are in fact very short. Depending on the waypoint type, between 40 percent and 70 percent of the durations are below one minute. This means, for example, that unaffected waypoints are consistently *seconds* faster to search. For "action" waypoints, there are not as many observations which results in a more discrete cumulative distribution function. Interestingly here assists take less time to complete than shelter.

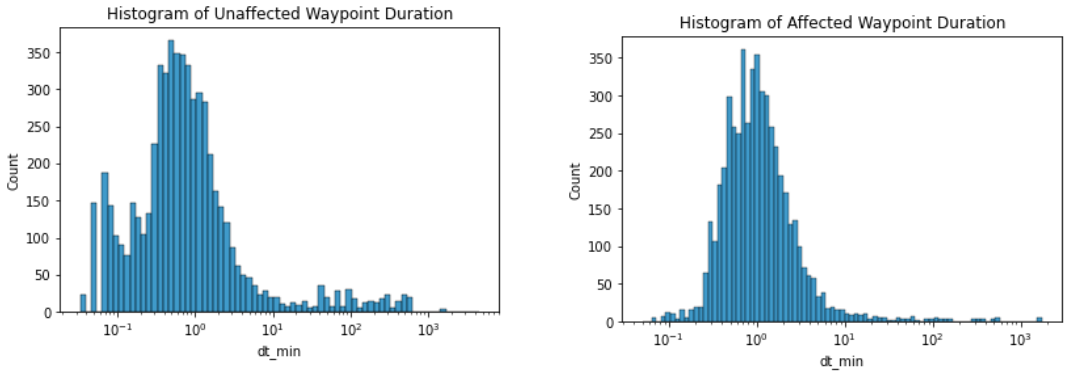

Figure 29. Histograms of waypoint durations for unaffected and affected waypoint types.

Overall, all of the distributions show a heavy tail which is why the x axis is presented in log scale. Almost 300 observations had a duration longer than two hours. Although it is unclear why, it is thought that it could be attributed to user error in logging the durations or a large travel time between waypoints. Figure 29 shows this heavy tail for the affected and unaffected waypoint types. It also illustrates the unaffected waypoint's unique distribution which has a smaller peak in waypoints with close to 0 duration and significantly more observations with durations greater than 100 minutes.

Search Path Analysis

An alternate approach to examining search duration is to examine the full path taken by each team each day. Each path will have a total duration and count of each type of waypoint encountered. By aggregating across the multiple waypoints in a path, we can potentially characterize the searches to see if they focus on particular types of severity.

asset_other	assist	block	destroyed	evac	extra21	extra22	followup	hazmat	icp	major	minor	other_haz	search	send_loc	shelter	staging	unaffected
0.0	0.0	0.0	1.0	0.0	0.0	0.0	0.0	0.0	0.0	0.0	188.0	0.0	0.0	0.0	0.0	0.0	40.0

Figure 30. Sample path detailing the quantities of each type of waypoint encountered.

When presented like this, each path can be visualized as a vector with each waypoint type representing a separate dimension. In this case the direction can be thought of the distribution of waypoint types encountered on the path and the magnitude can be considered a measure of the number of waypoints encountered. By using principal component analysis (PCA), we can plot the data in a lower dimensional space and better observe relationships in the data.

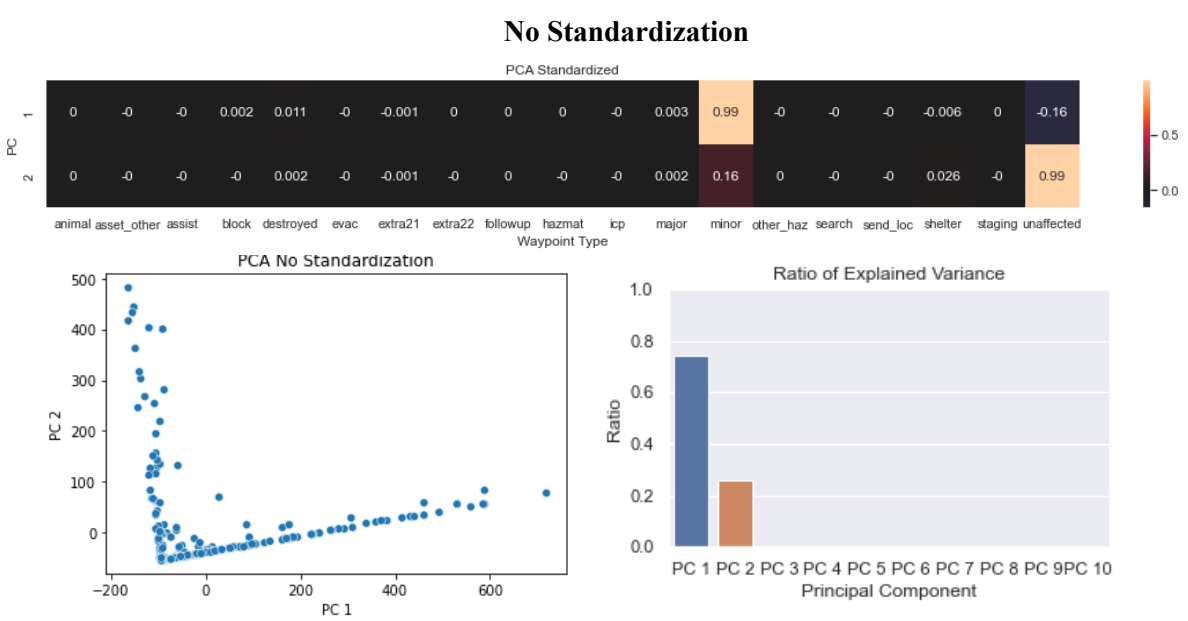

Figure 31a. (Top) First two eigenvectors of Hurricane Laura non-standardized path data. Figure 31b. (Bottom Left) Plot of search paths according to the first two principal components. Figure 31c. (Bottom Right) Ratio of explained variance for the first 10 principal components.

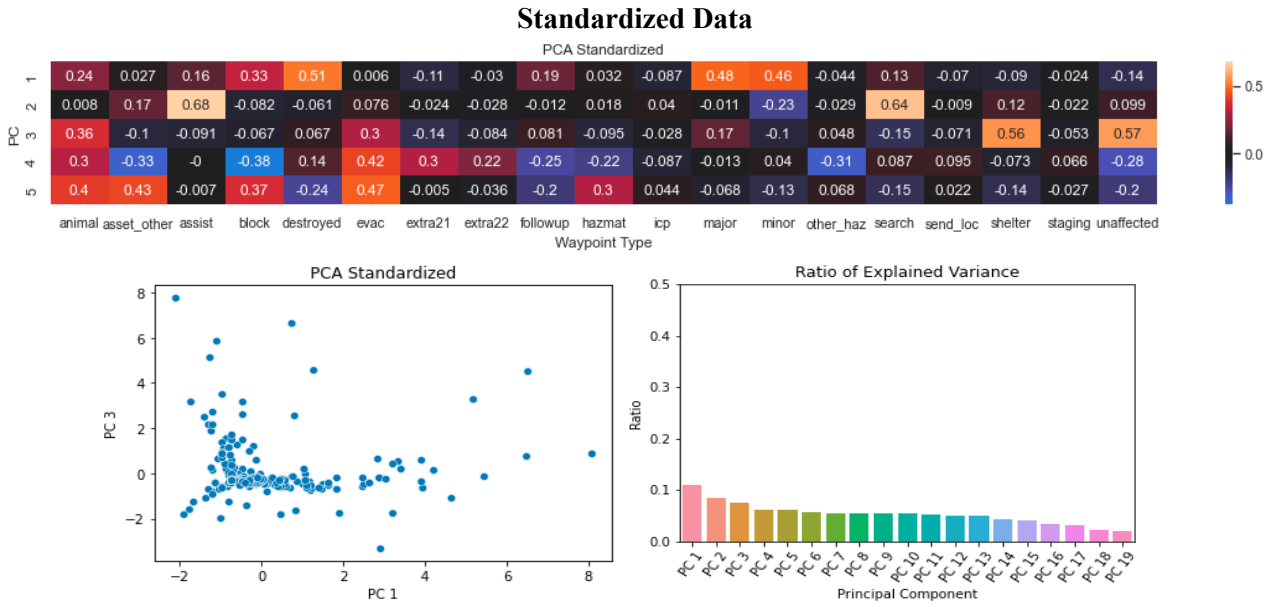

Figure 32a. (Top) First two eigenvectors of Hurricane Laura standardized path data. Figure 32b. (Bottom Left) Plot of search paths according to the first two principal components. Figure 32c. (Bottom Right) Ratio of explained variance for the first 10 principal components.

Initial PCA on the non-standardized path data (Fig. 31b) shows some structure present. Points align either along PC1 or PC2 forming an "L" shape corresponding to either having a large number of "minor" waypoints or "unaffected" waypoints. These variables are to be expected as principal components since both categories are present in large quantities in the data however, the lack of points with a large number of both categories together is unexpected. This trend carries over into the PCA for the standardized data. For the standardized data, the eigenvectors (Fig. 32a) show groups of related waypoint types. PC 1 is largest when there are a large number of minor, major, destroyed, and block waypoints present in a path indicating that there is structural damage present along the route. PC2 on the other hand is largest when there are search and assist waypoints present. Finally, PC3 is largest when there are unaffected and shelter waypoints present. When PC1 is plotted against PC3, the same "L" shape is subtly present. In this regard, further work is required to deduce. Admittedly, although these linearities are present, further work is needed to deduce if these patterns are exploitable information regarding search decisions or are a consequence of either the data collection process or the storm itself. Also, there is the open question regarding the flat profile of the ratios of explained variance (Fig. 32c) despite the observed structure. This could be due to having a large number of uncorrelated variables in addition to some of the data lying along orthogonal axes. Additional work would explore pruning or consolidate some of the features and observing the new output.

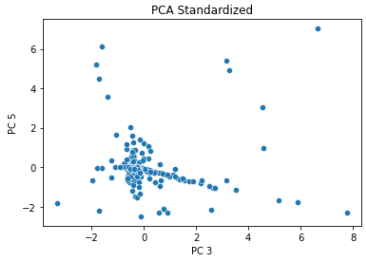

Figure 33. Another example of linearities found in the transformed standardized path data.

Simple Predictive Models

Although path search time is coupled with travel time between waypoints, preliminary work may still be done on estimating the search time of a path. Assuming that the total search time across all waypoints encountered on a path scales linearly with the number and type of waypoints encountered, we are able to create two simple models that predict the search time of a path. The first model is a linear regression fit to the path vectors (Fig. 30) and their corresponding total path time. The output of this model is a list of coefficients for each waypoint, roughly corresponding to the search time for that type of waypoint, and an intercept term which can be interpreted as a fixed overhead search time assigned to all paths. The model was fit to 60 percent of the data from the storm and its predictions plotted against the test set which was the remaining 40 percent. The coefficients are constrained to be positive to reflect positive time.

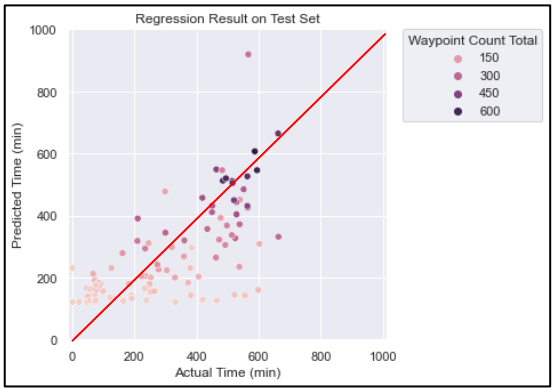


```
Intercept 120.07

animal 43.67
asset_other 106.92
assist 0.0
block 11.51
destroyed 0.0
evac 70.6
extra21 6.76
extra22 0.0
followup 0.0
hazmat 92.37
icp 0.0
major 13.83
minor 0.71
other_haz 0.0
search 0.0
send_loc 111.16
shelter 7.68
staging 0.0
unaffected 1.0
```

Figure 34. Regression Prediction results (left) with regression coefficients (right).

Above is the regression fit to the paths initiated after Hurricane Laura. For reference, the red line represents where the prediction and the actual time are equal, and the hue of the points indicates how many waypoints were encountered on that path. The scatterplot shows that the regression largely underpredicts a path's search time. In addition, it is apparent that there is a large variance in actual search time when waypoint count total is small which could indicate that the geography of the area and search route taken significantly affect the times.

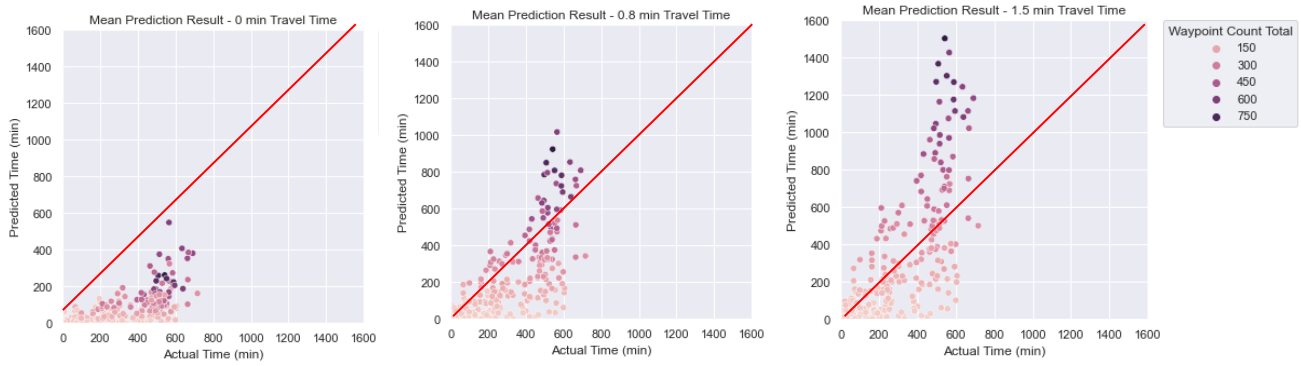

Figure 35. Mean Prediction results for varying assumed travel times between waypoints.

The second simple model is to calculate the average elapsed times for each type of waypoint and multiply them by their respective counts in each path. Assuming there exists some fixed "per waypoint" travel time, an additional term can be added that multiplies with the waypoint count to account for the added travel time. Above are various plots using different values for this fixed travel time. The points get scaled vertically as the per waypoint travel time increases. For paths with a large number of waypoints, this means

overestimating the search time. Overall, this again supports the inclusion of geographic and routing data towards the search time estimates.

Machine Learning Approaches

Exploratory work was done in leveraging machine learning techniques to predict the search time for a group of structures based on the damage of those structures. Significant effort was required to clean the data, as many entries contained incomplete information. For example, an entry missing the Squad ID would not be able to be aggregated with other activity by a squad and was eliminated from the training data.

Two models were developed: a Random Forest model and a custom Neural Network model. Both models performed similarly when comparing predicted values to observed values for time spent at any given structure, but the nature of the data collected challenged the meaningfulness of these predictions. Specifically, for situations when squads would enter a batch of structures, their time values would all be within seconds of each other. The models being trained on such data results in predictions that are true relative to the training data but not accurate in the real world.

As data collection becomes a more accurate reflection of the search team's action in space and time, and more of this data exists, it is recommended that a deep learning model be explored as an option.

Conclusion

Overall, many facets of the data were examined to look for exploitable trends. Firstly, Hazard data was found to be informative of the type of USAR waypoint categories encountered along a search path. These waypoint categories were then shown to have distinct search time distributions that, in turn, contribute to the total search time of a given path. When the paths themselves were analyzed using PCA, it appeared to show that paths either encountered damage or did not at all although this interpretation would require further work to support concretely. Finally, two models were constructed to predict the search time of a path given a vector of its encountered waypoints. The models, which demonstrated some predictive capacity, prove that waypoint data alone is insufficient and that geography and search routing must be incorporated as well for better performance.

7.8 SEARCH AREA SEGMENTATION

Automating the intuitive segmentation of an urban area is a challenging task. The team explored several different approaches, before finding the proposed solution.

7.8.1 Genetic Algorithm

Borrowing concepts from evolution, a genetic algorithm defines a problem in terms of "genes" and a goodness metric. A population of solutions is allowed to progress through gene "mutations" and "crossovers". Solutions are evaluated by the goodness metric, and the best solutions are allowed to continue

to the next generation. This approach provided poor initial results, and the time required exceeds operational constraints.

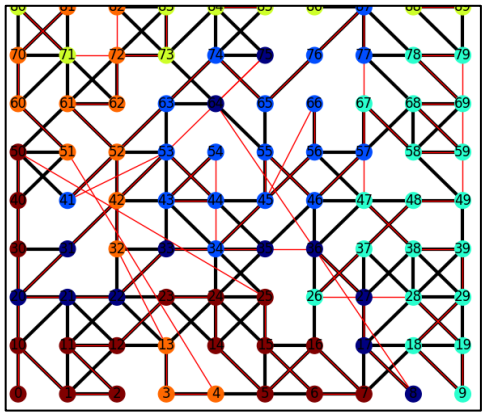

Figure 36. Genetic algorithm solution example.

7.8.2 K-Means Clustering

In this approach, for the area of interest, a set of points are specified. The Voronoi diagram is found, which is the set of polygons for which every point in that polygon is closer to the center than to the center of the neighboring polygons. In GIS terms, this is also known as Thiessen Polygons. Find a new center for each polygon based on the number of points in the polygon and their distance to the center. Repeat until there are an equal number of structures in each cluster. This approach is fast to run and simple to implement but does not respect geography or the rules of wide area search.

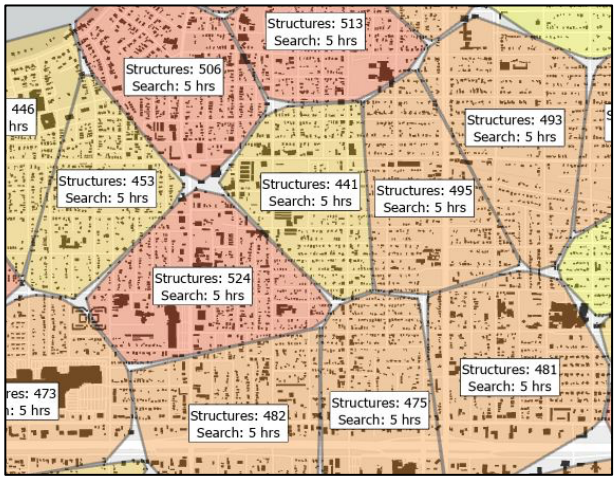

Figure 37. k-Means Clustering sample output.

7.8.3 Division Filtration

For a bounded area, find the outer edges and points on the edge that are the ends of roads. For some number of edge points, find the edge point that is most directly on the opposite side and find the least cost path between these points. Do this vertically, and also horizontally. The regions bounded by the horizontal and vertical lines create candidate search segments. Results adhere to roads but do not create equally sized segments.

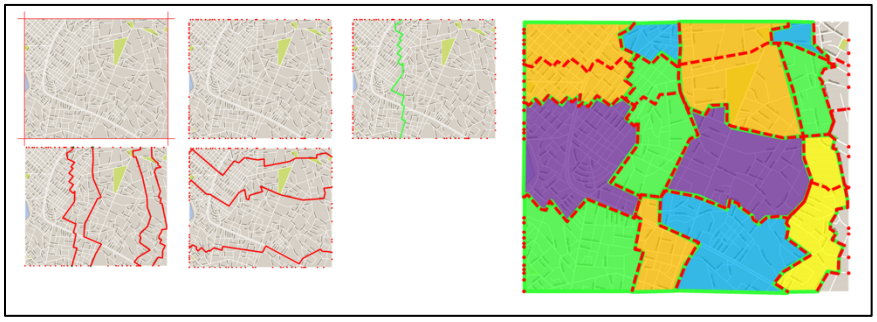

Figure 38. Division Filtration output example.

This page intentionally left blank.

APPENDIX B: A BAYESIAN PROBABILISTIC MODEL FOR ESTIMATING BUILDING DAMAGE DISTRIBUTION FROM FORECASTS

Jeffrey Liu, Chad Council*
Humanitarian Assistance and Disaster Relief Systems
MIT Lincoln Laboratory
Lexington, MA 02421
jeffrey.liu@ll.mit.edu , chad.council@ll.mit.edu

Abstract

Estimating the distribution of building damage from forecasted hazards can enable more effective urban search and rescue (USAR) planning and operations. Our work uses Bayesian probabilistic modeling to estimate the distribution of building damage levels from forecasted hazard scores. We leverage data on building damage collected from FEMA USAR teams during wide area search operations. Our results validate the performance of the FEMA hazard forecasts predictions for Hurricane Ian in 2022, and also quantitatively characterizes the distribution of building damage for each forecasted hazard level.

1 Introduction

Estimating the distribution of building damage from forecasts is a critical tool for the effective application of urban search and rescue (USAR) operations. Such estimations provide invaluable insights into the potential impact of natural disasters or catastrophic events on urban infrastructure, enabling emergency responders to strategically allocate their resources. By understanding which areas are likely to experience severe structural damage, search and rescue teams can prioritize their efforts, ensuring a more efficient and targeted response.

Emergency management agencies, like the Federal Emergency Management Agency (FEMA) in the United States, may put together forecasts of expected hazard levels prior to major tropical storms. These hazard levels are based on forecasted storm tracks, and can be combined with information such as exposure and vulnerability to help prioritize and prepare for disaster response. However, these hazard levels are usually reported as a ranking or index that provide relative comparison of hazard, without providing concrete estimates of impact. While this is useful for prioritizing areas for response, more concrete information, such as the distribution of building damage levels—how many buildings will be destroyed, majorly damaged, etc.—can allow for more granular planning.

We formulate a Bayesian probabilistic model of expected damage distributions for various levels of forecasted hazard using data reported by FEMA USAR teams during wide area search and rescue operations following Hurricane Ian in 2022. We validate the forecasted hazard scores provided by FEMA, and quantitatively characterize the building damage level distributions for each hazard score.

*DISTRIBUTION STATEMENT A. Approved for public release. Distribution is unlimited.
This material is based upon work supported by the Department of the Air Force under Air Force Contract No. FA8702-15-D-0001. Any opinions, findings, conclusions or recommendations expressed in this material are those of the author(s) and do not necessarily reflect the views of the Department of the Air Force.

Preprint. Under review.

Related Work

Bayesian probabilistic modeling is based on Bayesian probability theory, which provides a formal way to update beliefs about a system or phenomenon as new data becomes available. Within the Bayesian paradigm, probabilistic models allow for the incorporation of prior knowledge and domain expertise while providing a natural mechanism for quantifying and propagating uncertainty throughout the modeling process. Bayesian probabilistic models represent systems through probability distributions over the model parameters and latent variables. These models are particularly valuable in scenarios where data is limited, noisy, or exhibits intricate dependencies (1). Computational techniques such as variational inference (2) and Markov chain Monte Carlo (3) provide numerical tools to enable approximate inference on complex models and large datasets.

The ability of Bayesian probabilistic modeling to capture uncertainty and incorporate expert knowledge lends itself to search and rescue applications, where information is often limited, there are many sources of uncertainty, and experiential prior knowledge of first responders is a key element of decision making. Notable applications of Bayesian models in SAR applications include Davey et al.'s documentation of the various Bayesian methods used in the search for lost flight MH370 (4). Similar work has been done to model the behavior of missing persons, such as in (5). In (6), Norrington et al. construct a Bayesian network to model the decision making processes of the UK Coastguard's SAR operations, and use it to identify potential causes of unreliability.

2 Data

2.1 Urban Search and Rescue Waypoint Dataset

We acquired a set of GPS waypoint data from FEMA USAR teams, who have been tracking their building evaluation and clearing times for several years (7). The process of collecting this data is a relatively new part of the search and rescue team workflow, and its introduction has had some hiccups, resulting in data that required significant cleaning. The data collected during these responses consist of an ordered list of observations, indicating the time, location, and team associated as well as details of the observations. We refer to each observation as a "waypoint." Each waypoint can be one of may different types of observations, including a building damage level assessment, interaction with a survivor, documentation of an environmental hazard, interaction with an animal, among others. For this project, we focused on waypoints associated with building damage assessments. The building damage levels are coded as one of the following five categories, in order of increasing damage: unaffected, affected, minor, major, and destroyed. When we refer to a building's "damage level," we are referring to its classification in the aforementioned categories. In this paper, we focus on the search and rescue operations in the Fort Myers/Cape Coral area following Hurricane Ian in 2022. Figure 1b illustrates the distribution of building damage assessment waypoints in the dataset.

2.2 TEMPO Data

Prior to storm landfall, FEMA produces a hazard and impact estimate called the Tool for Emergency Management Prioritization and Operations, or TEMPO (8) (formerly known as Priority Operations Support Tool, or POST (9)). TEMPO is defined on the US National Grid (USNG) 1 km $\times$ 1 km grid, which is the grid reference system used for all land-based search and rescue activities in the US (10). For each cell, a numeric hazard score is assigned based on the anticipated hazard level of the event, with higher scores corresponding to more expected damage. The hazard ranking is then combined with social vulnerability information to create an overall prioritization index for each grid cell.

The TEMPO tool has gone through many iterations, and has revised its rubric and scale for each of the storms that we examine. Hurricane Ian in 2022 represents the most recent event that we have both TEMPO and USAR waypoint data for. The TEMPO hazard score is an integer value ranging between 1 and 20, where 1 represents the least severe, and 20 represents the most severe expected damage. Figure 1a illustrates the distribution of hazard scores for the area of interest.

To combine the USAR waypoint data with the TEMPO data, we performed a spatial join to annotate each USAR building waypoint with its respective USNG cell ID and associated TEMPO hazard score. Figure 1b illustrates the distribution of USAR building observation waypoints in the area of interest. In the data, we only observed USAR building waypoints in grid cells with hazard scores

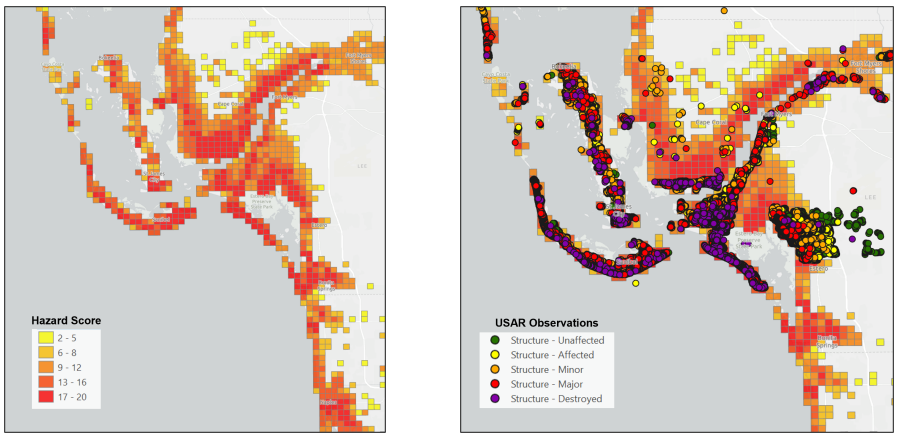

(a) (b)

Figure 1: Maps of Hurricane Ian TEMPO and USAR waypoint data

scores between 9 and 20. We note that not every grid cell that received a forecast had associated waypoint data; this may be because USAR teams were not tasked for those areas, or data was not recorded. In addition, there are some building waypoints that were recorded in areas where a TEMPO forecast was not generated. This may be a source of sampling bias, and we discuss this further in Section 4.

We aggregated each grid cell by counting the number of buildings for each damage level. Each row of the dataset thus contains the hazard score, the USNG grid identifier, the number of buildings of each damage level, and the total number of buildings in the cell. The data set has 436 rows, representing as many square kilometer grid cells. A few example rows of the data are included in Table 1 for illustration.

haz_score	usng1km	destroyed	major	minor	affected	unaffected	n_buildings
9	17R LK 5891	0	1	0	0	0	1
9	17R LK 5898	0	7	0	0	0	7
...	...	...	...	...	...	...	...
20	17R MK 1530	2	215	86	27	9	339
20	17R MK 1628	0	194	42	0	39	275

Table 1: Example data from the joined TEMPO and building damage dataset

3 Model

3.1 Formulation

In this section we discuss the process of estimating the distribution of building damage level based on storm impact forecasts. Varying levels of building damage will affect the expected time required to perform USAR operations, as buildings with greater levels of damage may be more difficult to navigate as well as increased likelihoods of individuals requiring assistance.

Our task is to estimate, for a given TEMPO hazard score, the expected distribution of damage in terms of the fraction of buildings in each cell corresponding to the respective damage levels. To achieve this, we constructed a Bayesian Probabilistic Graphical Model (PGM) using PyMC (11). We model the process as a Dirichlet-Multinomial model (12), where the distribution of building damage levels for each USNG cell are draws from multinomial distributions with priors drawn from a multivariate Dirichlet distribution. The process is modeled as such: for a given hazard level, a vector of probabilities is drawn from a Dirichlet distribution; these probabilities instantiate a Multinomial distribution, from which a realized distribution of counts of building damage levels is drawn.

We choose to model the process as Dirichlet-Multinomial as opposed to just a Multinomial process to capture the uncertainty in building distributions of a given forecast level. For example, two grid cells with the same forecasted hazard score score may have very different observed damage distributions based upon the realized track of the storm. A Multinomial process with a fixed probability distribution

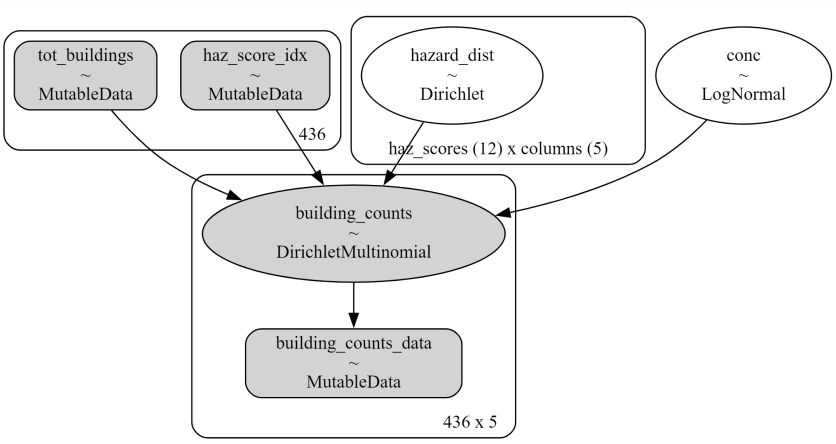

Figure 2: Probabilistic graphical model diagram illustrating the Dirichlet-Multinomial model for estimating building damage distribution from TEMPO forecasted hazard scores

for a given hazard score would not be able to capture this variation. Placing a Dirichlet prior on the multinomial probabilities allows us to model this uncertainty.

Figure 2 illustrates the model. The `hazard_dist` variable is drawn from a `num_hazard_scores` $\times$ `num_damage_levels`-dimensional Dirichlet distribution, where `num_hazard_scores`$= 12$, for each hazard score between 9-20, and `num_damage_levels`$= 5$ for each of the damage categories: unaffected, affected, minor, major, and destroyed. We also include a `conc` concentration parameter for the Dirichlet-Multinomial drawn from a Log-Normal prior distribution with $\mu = 1, \sigma = 1$.

From the data, we take the total number of buildings per grid cell, `tot_buildings`, and the projected hazard score converted to an index from [0,11], `haz_score_idx`, as input variables. The variable `tot_buildings` determines the number of draws from the Multinomial distribution, and `haz_score_idx` selects which dimension of the `hazard_dist` Dirichlet prior to draw the Multinomial probabilities from. Each hazard score dimension of the Dirichlet prior is treated independently, so only the dimension corresponding to the observed variable is updated in each update step. The observed variable, `building_counts_data`, is a `num_data_points` $\times$ `num_damage_levels`-dimensional array, where each row is the observed number of building counts of each damage level. The model was fit using PyMC's No U-Turn Sampler for Hamiltonian Monte Carlo (11). We took 16,000 samples, with the first 8,000 used for tuning.

3.2 Results

We are most interested in the `hazard_dist` variable, as it is what characterizes the distribution of building damage for each forecasted hazard level. Recall that the `hazard_dist` variable is the Dirichlet prior which provides the probabilities for each cell's Multinomial distribution from which the realized damage observation is drawn. Thus, the posterior of `hazard_dist` characterizes the expected proportion and variance in damage levels for each hazard score, given the observed data.

For the sake of brevity, we present only the posterior distributions for the lowest and highest observed hazard scores (9 and 20, respectively) in the body of the paper; these are illustrated in Figure 3. The full posterior for all hazard scores is included in the supplemental material.

The mean of the posterior for a given hazard score and damage level represents the expected fraction of buildings observed at that damage level and hazard score. The width of the posterior, which we report using the 94% high density interval (HDI), represents the expected variation in building counts at that damage level for a given hazard level.

We can compare the change in posterior across different hazard levels to characterize differences in expected damage distribution as hazard levels change. Figure 3 present the posteriors for the lowest and highest observed hazard scores, 9 and 20, for comparison. A higher mean for a given damage level represents that we expect a larger fraction of the buildings to be at that damage level, and a

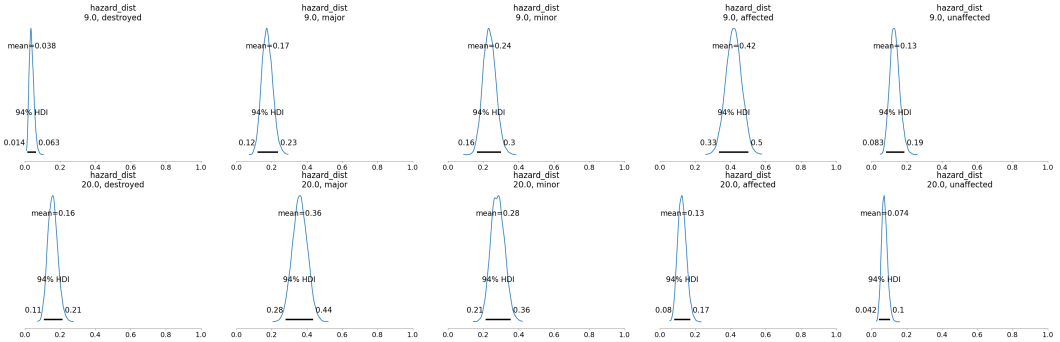

Figure 3: Posterior distributions for the `hazard_dist` variable for hazard scores 9 (top row) and 20 (bottom row). Columns represent building damage level from most severe (destroyed) on the left to least severe (unaffected) on the right. The mean and 94% high density intervals are indicated on each subplot.

wider posterior represents that we expect more variation in the counts for that building damage level across different cells.

From this comparison, we can see that when going from hazard level 9 to 20, there is a clear decrease in the expected fraction of low severity damage levels: the fraction of buildings unaffected decreases from 13% to 7%, and those affected decreases from 42% to 13%. Conversely, we see increases in the higher severity damage levels: the fraction of buildings with minor damage increases from 24% to 28%, those with major damage increase from 17% to 36%, and those destroyed increase from 3.8% to 16%. The relative changes in fraction for the higher severity damage levels also increase with severity, with minor, major, and destroyed damage levels increasing 1.17 times, 2.12 times, and 4.21 times respectively. The variance of the higher damage levels also increase with hazard scores, with minor, major, and destroyed having wider distributions, and affected and unaffected having narrower distributions.

4 Discussion

Our effort is the first to validate and characterize the predictions of the TEMPO hazard model and convert the unitless hazard scores to real expected impacts on building damage in a disaster. Our analysis validates the TEMPO hazard score forecasts by demonstrating that the higher scores do indeed correspond to greater proportion of buildings experiencing more severe damage. However, beyond validating this notion qualitatively, we are able to assign precise expectations of the fraction and variance of buildings at each damage level for a given hazard score forecast. This could be used to provide more precise calibration of the TEMPO hazard score for future iterations.

Our model also allows us to generate predicted distributions of damage for a given hazard score, allowing for better-informed disaster planning and response efforts, such as pre-allocating resources and tasking USAR teams. This approach can be easily extended to other forecasted risk/hazard models and impact measures to characterize expected impacts for a given forecast. The requirements would be that the forecasts be able discretized onto regular spatial cells, quantized into discrete categories of risk, and that the impacts be able to be represented as discrete categories.

The TEMPO forecast has gone through several iterations, and thus it was not possible for us to directly compare multiple historical storms due to changes in methodology. However, as the TEMPO product matures, we expect that the methodology will be standardized, and predictions from one storm can be directly compared to those from another. As such, we hope to be able to validate our approach by comparing models fitted on separate storms to see if there is agreement on their predictions.

We note that there is a potential source of bias in using the data from USAR waypoints to estimate the damage distribution, in that the data is collected in areas where the storm effects were severe enough that a USAR team was tasked to perform a wide area search. Consequentially, the estimates of damage distribution may be biased toward higher levels of damage than if the cells were sampled randomly. Since USAR data for areas that were not tasked do not exist, we would need to use

an independent data source to identify whether there is a significant bias in using USAR-recorded building damage levels to estimate the building damage distributions from forecasts. Potential sources of additional data include estimates from remote sensing, as well as independent damage assessments from emergency management and insurance agencies.

The estimated distribution of building damage levels could be integrated into downstream tasks—for example, estimating the time required for USAR to clear a given grid cell. Such estimates could improve USAR operations by giving better estimates of effort for a given tasking, allowing emergency managers to better predict the resources and personnel required to allocate to each region.

References

[1] Daphne Koller and Nir Friedman. *Probabilistic graphical models: principles and techniques*. MIT press, 2009.

[2] David M. Blei, Alp Kucukelbir, and Jon D. McAuliffe. Variational inference: A review for statisticians. *Journal of the American Statistical Association*, 112(518):859–877, apr 2017. doi: 10.1080/01621459.2017.1285773. URL https://doi.org/10.1080%2F01621459.2017.1285773.

[3] S. Brooks, A. Gelman, G. Jones, and X.L. Meng. *Handbook of Markov Chain Monte Carlo*. Chapman & Hall/CRC Handbooks of Modern Statistical Methods. CRC Press, 2011. ISBN 9781420079425. URL https://books.google.com/books?id=qfRsAIKZ4rIC.

[4] S. Davey, N. Gordon, I. Holland, M. Rutten, and J. Williams. *Bayesian Methods in the Search for MH370*. SpringerBriefs in Electrical and Computer Engineering. Springer Singapore, 2016. ISBN 9789811003790. URL https://books.google.com/books?id=XNtCDwAAQBAJ.

[5] Denis Reilly. Bayesian networks for decision support in emergency response: A model for missing person investigations. In Denis Reilly, editor, *Contemporary Issues in Information Systems*, chapter 3. IntechOpen, Rijeka, 2022. doi: 10.5772/intechopen.105047. URL https://doi.org/10.5772/intechopen.105047.

[6] Lisa Norrington, John Quigley, Ashley Russell, and Robert Van der Meer. Modelling the reliability of search and rescue operations with bayesian belief networks. *Reliability Engineering & System Safety*, 93(7):940–949, 2008. ISSN 0951-8320. doi: https://doi.org/10.1016/j.ress.2007.03.006. URL https://www.sciencedirect.com/science/article/pii/S0951832007001032. Bayesian Networks in Dependability.

[7] Jared Doke. SARCOP Data Dictionary, 4 2023. URL https://www.arcgis.com/home/item.html?id=da089975974d45a3826e246be2d10be6.

[8] New Light Technologies and FEMA. TEMPO. URL https://tempo.nltmso.com/?bbox=-124.966%2C25.454%2C-66.344%2C51.106.

[9] Ran Goldblatt and Adam Barker. Prioritizing Operations Support Tool (POST) deep dive and demo, 2018.

[10] National Search and Rescue Committee. *Land Search and Rescue Addendum to the National Search and Rescue Supplement to the International Aeronautical and Maritime Search and Rescue Manual*. dbS Productions LLC, 2011.

[11] Abril-Pla Oriol, Andreani Virgile, Carroll Colin, Dong Larry, Fonnesbeck Christopher J., Kochurov Maxim, Kumar Ravin, Lao Jupeng, Luhmann Christian C., Martin Osvaldo A., Osthege Michael, Vieira Ricardo, Wiecki Thomas, and Zinkov Robert. Pymc: A modern and comprehensive probabilistic programming framework in python. *PeerJ Computer Science*, 9: e1516, 2023. doi: 10.7717/peerj-cs.1516.

[12] James E. Mosimann. On the compound multinomial distribution, the multivariate β- distribution, and correlations among proportions. *Biometrika*, 49(1/2):65–82, 1962. ISSN 00063444. URL http://www.jstor.org/stable/2333468.

APPENDIX C: CITY PARTITIONING TO ENABLE BALANCED EMERGENCY RESPONSE EFFORTS

Dieter W. Schuldt
Humanitarian Assistance and Disaster Relief Systems Group
MIT Lincoln Laboratory
Lexington, MA 02421
dieter.schuldt@ll.mit.edu

Abstract

When a group of responding teams are tasked with emergency search and rescue or aid distribution in a region, that region needs to be partitioned into a set of sub-regions to deconflict the teams and maximize their efforts. This paper presents a method for dividing a city into a set of partitions that present approximately identical workloads. This method takes a graph based approach, representing cities by their road network and with weighting based on the number of adjacent structures. The algorithm provided is flexible enough to accommodate the complexities of city street networks. Critically, in order to improve user adoption this method attempts to formalize current intuition-based methods instead of focusing on pure optimization. Application of this algorithm to a segment of a real city is presented.

1 Introduction

Wide area search and rescue (the search for an unknown number of targets over a large area) is a key component of response to hurricanes, fires, earthquakes, and other natural disasters. Because of the immensity of this task, the common practice is to divide up the impacted region into a collection of sub-regions that can be searched by small teams.

The current method for this division uses human intuition and experience to slice up the search area. This may result in reasonably balanced partitions, but it lacks any sort of rigor that could be used for analysis. Automatizing this process opens up the process to scrutiny and affords future improvement.

There are other scenarios beyond search and rescue where this capability could prove beneficial. Distribution of aid is frequently performed in similar circumstances as wide area search and rescue. Being able to more rapidly disburse aid has the potential to reduce the required manpower and improve the experiences of the beneficiaries. Balanced city division could also be incorporated into data collection tasks such as the census and door-to-door disease surveillance.

This task is complicated by the fact that cities are not laid out on perfect grids, and disasters don't comport with municipal boundaries. Any solution has to be flexible enough to deal with the peculiarities that bedevil cities. Valleys, mountains, waterways, industrial zones, and more lead to roads that swirl, end, and split. The method presented here has been tested in many circumstances, but almost certainly there are cities that are in such disarray that it will have to be adapted.

The objective of the method presented here is not just to perform equal partitioning, which is a well defined task in computer science[3, 1], but to do it in service of also keeping the total time to traverse all arcs in the graph low. Compact (rectangular), well-connected regions can be used as a heuristic for low coverage times[6]. As such, this method aims to create divisions that are approximately equal in weight, but which also have a compact footprint and don't cross waterways or highways. This helps to maintain dense connections within the regions. In general, solving the k-person arc traversal problem is NP-hard[5], meaning it is not practical for wide area search. However, the

method proposed here has the added benefit of producing regions that match human intuition about fair partitions. Understandability has been identified as a factor in user adoption of technology[7].

2 Methods

The objective of this algorithm is to take a connected road network and return a partition of that road network such that each part of the partition will take the same amount of time to search. This comes with the added restriction that the parts conform to user expectations about shape, namely that they not cross rivers or highways, that they are rectangular, and that they follow streets. By applying the algorithm to a collection of connected road networks we can create a search plan that covers the city or other region of interest.

In the proposed method we take an iterative approach, applying a splitting function f that accepts a connected road network and a number of teams and returns two connected road networks, each with a complementary fraction of the teams assigned to the initial connected road network. Consider a connected graph G and number of teams N. Then, $f((G, N)) = \{(G_1, N_1), (G_2, N_2)\}$. This is depicted in figure 1. If N_i is 1, then we have succeeded in defining a region for one team, and no further processing of that part is necessary. Once all of the parts have $N_i = 1$, the procedure is complete.

The splitting function consists of a series of key steps:

1. Find the boundary of the graph
2. Find a path from one point on the boundary to another that divides the region equally according to some metric
3. Return the two regions that exist on either side of the path

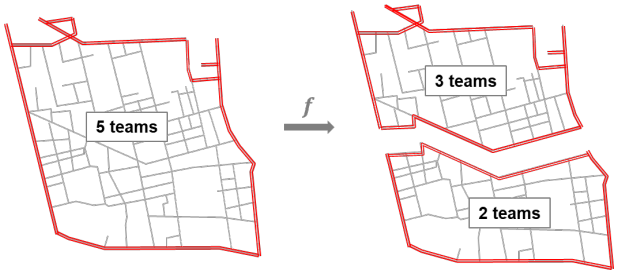

Figure 1: A connected region and set of teams is divided into two connected regions and two sets of teams. The boundary of the region is depicted in red.

As previously stated, the objective of this research is to provide a tool for disaster managers to efficiently distribute the resources that they are given. In order for the tools to be adopted, it is not enough that the regions are optimized, they also need to conform to certain expectations that disaster managers have. Solutions that go on wild excursions (even if slightly more efficient) are unlikely to be trusted by responders.

To efficiently divide the labor, each team is given an equal amount of work. In this case we are focused on balancing the number of structures between regions, because we are assuming that the bulk of the time involved in the activity is spent at the structures and that it substantially outweighs any travel time.

Dividing a continuous density convex region into partitions such that each partition has an equal overall amount of weight is trivially accomplished, but in the case that we are investigating it is significantly more complex due to complications that arise on discrete spaces.

For the purposes of this analysis we will treat a search region as a graph $G = \langle V, E \rangle$, with vertex set V and edge set E. Edges represent roads, with vertices being intersections. Each edge (e_i) is decorated with the length of the edge $(e_{i,\ell})$, and the number of structures on that portion of road $(e_{i,S})$. Vertices are decorated with their $v_{i,x}, v_{i,y}$ location, which in our case are the latitude and longitude of the intersection. Assign the number of teams engaging in the search to N. The objective

is to find a "cut set" κ, consisting of edges $e_i \in E$, such that the graph resulting from removing them from G consists of exactly N connected components. Denote the number of connected components in a graph as $||G||$.

All of the edges that are highways or which cross waterways are removed. This will ensure that no partition crosses these boundaries. Removing these edges may result in a collection of components that are not connected to each other. For the rest of this analysis we will be focusing on a single connected component. Without loss of generality, this component can be any of the connected components. We will consider each of these connected components in turn, which when pieced together cover an arbitrary area. Going forward we will use G to refer the single connected component.

An optimal partitioning of G would require an exponential (in number of nodes) amount of time to calculate, meaning that it is impractical to find[2]. Instead, we will construct an iterative algorithm that bisects connected components. By repeating this $N - 1$ times we will arrive at a set of N connected components. Significant research has been done on the bisection problem[3], but these methods do not take into consideration the requirements set forward in our problem.

The first step in the process of partitioning is to find the perimeter of G. The algorithm for this is algorithm A1 in the appendix. For our purposes, the perimeter is the subgraph of G defined as the loop that has as the most nodes in its interior. For our purposes it also includes all nodes not contained by that loop (the tendrils that protrude from the loop). This process is rather involved because of how complex road networks are in real life. The essence of this algorithm is to treat the road network as a maze, and trace a path by keeping one hand on the wall at all times. The end result is a path that tightly encircles region.

Next we will partition the road space. The process of partitioning consists of finding a road path, called a "cut", that travels from one point on the perimeter to another point on the perimeter. At each iteration we will find the best cut from a collection of 4 potential cuts (two horizontal and two vertical). The optimality of the cut is based on balancing the "load" per team on either side of the cut. One of the simplest load metrics (and the one that we are using) is number of structures in the region, but this could readily be extended to the expected search time across the structures in the partition, or any number of other metrics.

The final step is to construct an algorithm that divides the connected road graph and number of teams into a set of search regions of approximately equal load. The main loop of algorithm A2 (Space division algorithm / Appendix) (starting at bullet 3) takes a connected road graph and returns two connected road graphs. This means that the output from each iteration can be treated individually as components of the form we started the algorithm with! This process is repeated until the number of teams assigned to each partition is 1.

Finding the cut that produces equal loads is accomplished using an iterated approach as well. This method, known as half splitting, finds the optimal cut by bracketing where that cut might be. For example, if we are trying to find a vertical cut, we initially cannot rule out any potential cut, so the bracket is places at the nodes with the smallest and largest longitude (x) values. Propose a cut at the midway between the brackets. Since we want to cut to follow the roads, we turn the vertical cut into a path on the road network. If the left side of the cut has more load than the right side of the cut, we know that the optimal cut lies to the right of the midway cut proposed before (otherwise it lies to the right). Thus, we can move the right bracket to the midway and repeat the process. At the end of this process there is a cut that approximates the optimal division of the region. This process is shown in figure 2.

By applying this method to each connected component, we will arrive at a partitioning of the entire region of interest. Each segment has approximately the same workload. Since finding the shortest path is the dominating term in the runtime of this algorithm the complexity is $\mathcal{O}(VE)$, a substantial savings on the NP-hard optimal assignment problem!

3 Discussion

To demonstrate this algorithm in practice, we provide an example performed on the city of Tampa, FL.

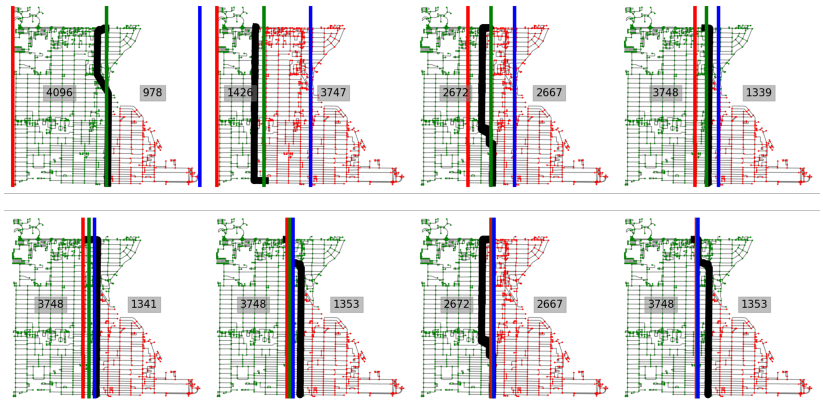

Figure 2: Iterations of the Space Division algorithm (A2), for a 3/2 split. (red) The left bound (x^-), (blue) the right bound (x^+), (green) the proposed cut ($m = (x^- + x^+)/2$), and (black) the shortest path cut (κ). The numbers identify how many structures are in each part. The result only differs from the desired load ratio by 7%

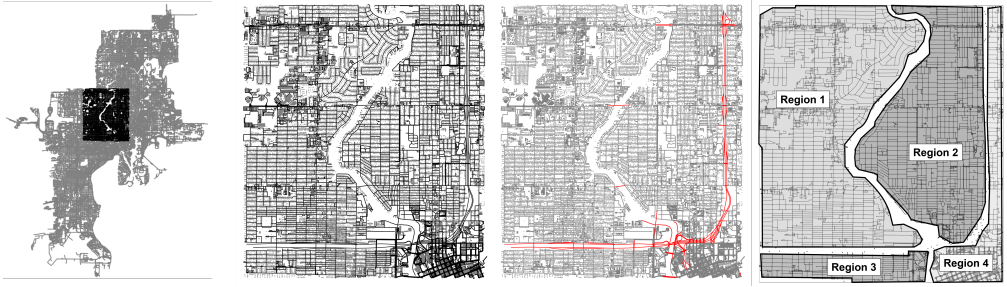

Figure 3: (left to right) The road structure of the city of Tampa, FL with a region of interest highlighted; Enlargement of the region of interest; The region of interest with bridges and highways highlighted; The connected regions produced from removing bridges and highways

As we see in Figure 3, the city of Tampa is comprised of a very large number of streets and has a highly irregular shape. Well start by selecting a bounding box for the area of search. This could be the entire city, but for ease of visualization we've limited it to a $0.05° \times 0.05°$ square, having an area of approximately $25km^2$. This region was selected because it exhibits many of the confounding factors identified as impediments to automated search area partitioning: irregular street structure, water features (both internally and on the boundary), and highways. After the bridges and highways are removed we are left with four connected regions that will be partitioned independently and then recombined. We'll choose 11 teams for the search of this area: 5 for region 1, 4 for region 2, and 1 each in regions 3 and 4.

The final partition is provided in figure 4. As can be seen, this partition has the desirable compactness that was identified as a requirement for user adoption.

At the end of partitioning the number of structures assigned to each team ranges from 930 to 2025. There are 17292 structures in the region of interest, which means that a completely equal division would assign each team 1572 structures. The outliers on either end (at 930 and 2025 structures) are 41% and 28% off of optimal, but 8 of the 11 teams are assigned within 15% of optimal.

4 Conclusion

This paper demonstrates a graph based approach to partitioning a city for balanced search and rescue response. The division is made on the basis of maintaining compact regions that do not bridge waterways or highways. This comports with the expectations of experts in search and rescue, who are ultimately the target audience of this work, and also works as a heuristic for optimal arc traversal

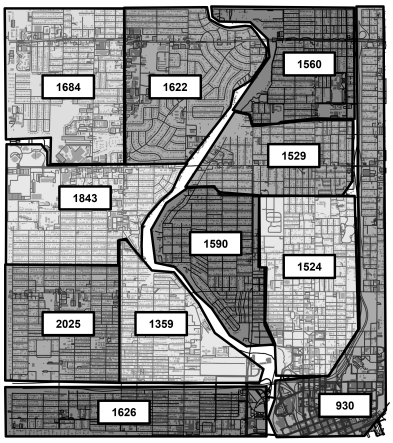

Figure 4: The complete partitioning of the ROI with 11 teams. Numbers indicate the building count in that part of the partition.

times. The developed algorithm is flexible enough to accommodate many of the peculiarities present in city road networks.

The end result is an algorithm that, in limited testing, is able to produce partitions that are generally within 15% of optimal. This has the potential to improve response times and add scientific rigor that can be used to add quantification to after action analysis. Human intuition will always be a critical part of the disaster response process, but tools like these are augmentations that allow responders to reach their full potential.

A number of improvements are still needed in future work. In this work, roads are all considered equally passable. Incorporating data about passability acquired during the search, or using remotely sensed data acquired before the search begins, has the potential to provide significantly better estimates of travel time and the amount of damage at each structure. The data that is currently available does not include information about the type of structure, in particular the number of people living in the structure. If this information becomes available, it has the potential to significantly alter the estimates of search times. The partitioning algorithm needs to be exercised over more regions. During development with the Tampa, FL dataset numerous modifications had to be made to the algorithm to account for unforeseen contingencies. It is expected that there will be additional complications that arise as it is tried in various locales. User testing needs to be performed to determine if this algorithm lives up to their expectations. Results also need to be compared to the human-drawn boundaries that are currently used. If automated partitioning doesn't provide a notable improvement, then there is no reason to force it into the already established workflow.

5 Acknowledgements

DISTRIBUTION STATEMENT A. Approved for public release. Distribution is unlimited.

This material is based upon work supported by the Department of the Air Force under Air Force Contract No. FA8702-15-D-0001. Any opinions, findings, conclusions or recommendations expressed in this material are those of the author(s) and do not necessarily reflect the views of the Department of the Air Force.

References

[1] Bruce Hendrickson and Tamara G Kolda. Graph partitioning models for parallel computing. *Parallel computing*, 26(12):1519–1534, 2000.

[2] Laurent Hyafil and Ronald Rivest. Graph partitioning and constructing optimal decision trees are polynomial complete problems. Technical Report Rapport de Recherche no. 33, IRIA – Laboratoire de Recherche en Informatique et Automatique.

[3] George Karypis and Vipin Kumar. A fast and high quality multilevel scheme for partitioning irregular graphs. *SIAM Journal on scientific Computing*, 20(1):359–392, 1998.

[4] Amgad Madkour, Walid G Aref, Faizan Ur Rehman, Mohamed Abdur Rahman, and Saleh Basalamah. A survey of shortest-path algorithms. *arXiv preprint arXiv:1705.02044*, 2017.

[5] Wen Lea Pearn. Solvable cases of the k-person chinese postman problem. *Operations Research Letters*, 16(4):241–244, 1994.

[6] Dieter Wolfgang Schuldt. *Application of Agent-Based Modeling to Problems in Humanitarian Assistance and Disaster Relief.* PhD thesis, Tufts University, 2022.

[7] Donghee Shin. The effects of explainability and causability on perception, trust, and acceptance: Implications for explainable ai. *International Journal of Human-Computer Studies*, 146:102551, 2021.

6 Appendix

In some cases it is useful to think of a node of the graph as a vector, in which case we will use the notation $\overrightarrow{v}$ to denote the vector running from the origin to node v. We will assume that $||G-T|| \leq N$. Because of this requirement, we will work with each connected component individually. Initially we have $\sum_i ||G_i|| = \sum_i N_i = ||G|| = N$ where G_i is a connected component of G. Define the number of structures in connected component G_i as $S_i = \sum_j e_{j,S}$, where a structure belongs to a graph if it is closer to an element of that graph than to any other graph in the set. Since each component has to have at 1 least team assigned to it, begin by placing one team in each connected component. Then, assign the remaining teams proportionally to the number of structures to be searched in that component. This means that the number of teams assigned to component G_i is

$$N_i = \left\lfloor (N - ||G||) \cdot \frac{S_i - \frac{S}{N}}{S - ||G|| \cdot \frac{S}{N}} \right\rfloor + 1 \tag{1}$$

Since teams have to be assigned in whole numbers, this may result in an under-utilization of available teams. As such, we assign the remaining teams to segments according to the disparity $S_i / \sum_j S_j - \lfloor S_i / \sum_j S_j \rfloor$. This assignment is not rigorously optimal, and can be adjusted in accordance with personal experience or other evidence of superior solutions.

Edges are also supplied with a type $(e_{i,T})$ where T belongs to the set $T := \{normal, highway, bridge\}$. To comport with disaster manager expectations, we will first remove all of the edges such that $T = \{e_i | e_{i,T} \in \{bridge, highway\}\}$.

Define a partition P of a space S as a set of sets such that for $P = \{p_1, ..., p_n\}$, $\bigcup_i p_i = S$ and p_i is connected. In the case of continuous spaces it is normally stated that a partition is only valid if the measure of $p_i \cap p_j$ is 0 $\forall i, j$. For the discrete space we will permit a partition as long as $p_i \cap p_j$ is a set of paths $\forall i, j$, where a path is a graph with exactly 2 nodes that have degree 1 and all other nodes have degree 2.

Define the "star" of v, $H = \langle V_H, E_H \rangle = v^* : G \to G$ as the subgraph consisting of all edges that contain v (and all vertices in those edges).

Define the the "quiver" of H, $Q(H) = Q(v_0^*) : E_H \to \mathbb{R}^{2 \times n}$ as the set of vectors $\{\vec{v_i} - \vec{v_0} | \vec{v_i} \in v_0^*\}$

(A1) Perimeter construction algorithm (G° is the perimeter of G)

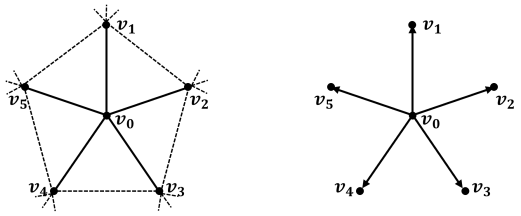

Figure 5: (left) The star of v_0 and (right) the quiver of v_0^*

1. Initialize:
   (a) $v_0 = v_i | v_{i,y} > v_{j,y} \forall j \neq i$
   (b) E°, and empty list
   (c) Set the perimeter vertex list $V^\circ = [v_0]$
   (d) $\vec{r} = (1, 0)$
2. While $v_1 \neq v_0$
   (a) Find $H = v_0^*$
   (b) Find $U = Q(H)$
   (c) Construct the set of clockwise angles between $\vec{h_i} \in U$ and r by calculating $\theta_i = atan2(dot(\vec{h_i}, \vec{r})/det(\vec{h_i}, \vec{r}))$, where $dot()$ is the dot product, and $det()$ is the determinant
      - if $\theta \leq 0$ then $\theta_i = \theta_i + 2\pi$
   (d) $\vec{e_1} = \underset{i}{\operatorname{argmin}}\ \theta_i$ (the edge vector associated with the smallest angle)
   (e) $\vec{r} = \vec{V}_{end} - \vec{v_1}$, where v_1 is the vertex associated with e_1.
   (f) Add $\vec{e_1}$ to the end of E°
3. Produce G° from E° by considering it as a subgraph of G

Given a boundary ϕ on a graph G, define the subgraph of G inside of ϕ as $\phi_G^\bullet$.

Define the load function $L : E \to \mathbb{R}$ defined as $L(\hat{E}) = \Sigma_{\hat{e} \in \hat{E}}(\hat{e}_S)$; that is, the number of structures in the partition.

As previously stated, the number of teams assigned to connected component i is N_i. We will consider vertical and horizontal cuts that produce divisions with $\lfloor N_i/2 \rfloor$ teams in one partition and $\lceil N_i/2 \rceil$ in the other. It would be possible to consider more possible divisions of the N_i teams, but in practice we have seen very little improvement when this is done.

Consider G° as an ordered list of points mod its length $G^\circ = (v_0, v_1, ..., v_n, v_0, ...)$. Define γ as an orders list of unique points, with $\gamma_0, \gamma_{end} = v_i, v_j$. Define the operation `separate(`G°`,`γ`)` that constructs two new lists:

$C_1, C_2 = \{v_1, ..., \gamma_0, ..., \gamma_{end}, v_{j+1}, ..., v_0\}, \{v_{i+1}, ..., v_{j+1}, \gamma_{end}, ..., \gamma_0\}$

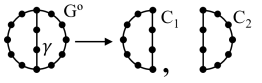

(A2) Space division algorithm

1. Given
   (a) Road graph $G = \langle V, E \rangle$
   (b) Number of teams N
2. Define $\Pi = \{(G, N)\}$
3. While the element with the largest number of teams in Π is > 1

(a) Find I such that $N_I > N_j \forall I \neq j$

(b) There are 4 different cuts that we will consider: two horizontal and two vertical (each with $\lfloor N_i/2 \rfloor$ in one half, and $\lceil N_i/2 \rceil$ in the other). Call these four cuts $\kappa_{H\uparrow}, \kappa_{H\downarrow}, \kappa_{L\leftarrow}, \kappa_{L\rightarrow}$. The following is written for a horizontal cut with the smaller number of teams in the upper portion, but is easily modified for the other cases.

i. Find x^+ (resp. x^-) the minimum (resp. maximum) value of $v_i, x | v_i, x \in V_I$

ii. Define $m = (x^+ + x^-)/2$

iii. While $\kappa \neq \kappa^{prev}$

A. Copy κ into κ^{prev}

B. Find the division κ and load ratio $LR = L(\alpha)/L(\beta)$ produced using Algorithm (A3)

C. Define $N_\uparrow = \lfloor N_I/2 \rfloor$ and $N_\downarrow \lceil N_I/2 \rceil$

D. If $LR \cdot N_\downarrow / N_\uparrow > 1$

- $x^- = m$
- $m = (x^+ + m)/2$

E. Otherwise

- $x^+ = m$
- $m = (x^- + m)/2$

(c) Choose the best cut κ^* from $\kappa_{H\uparrow}, \kappa_{H\downarrow}, \kappa_{L\leftarrow}, \kappa_{L\rightarrow}$ that minimizes $|1 - (min(L(a), L(b))/max(L(a), L(b))) * (\lceil N_i/2 \rceil \,/\, \lfloor N_i/2 \rfloor)|$, for a, b from `separate(`G°`,`κ`)`

(d) Assume G_a, G_b are the graph perimeters from `separate(`G°`,`κ`)`

(e) Replace (G_I, N_I) in Π with $(G_a^\bullet, \lfloor N^*/2 \rfloor), (G_b^\bullet, \lceil N^*/2 \rceil)$

(A3) Load ratio algorithm

1. Given
   - A graph: G
   - A level: m
   - A ratio: R
2. Find perimeter G° using Algorithm A1
3. Find the pierce points Γ where the horizontal line $y = m$ intersects G°
4. Construct the set of potential perimeters $\boxed{G}$
   (a) For each pair of pierce points (p_i, p_{i+1})
      i. Find the nodes (n, m) in G° closes to the pierce points (that is $D(n, p_i) < D(n_k, p_i)$ and $D(m, p_{i+1}) < D(n_k, p_{i+1}) \forall k$, where $D(i, j)$ is the distance from i to j)
      ii. Find the shortest path κ between n and m on G [4]
      iii. Construct the potential perimeters $\alpha, \beta =$`separate(`$G^{*\circ}$`,`κ`)`
      iv. Add (α, β, κ) to $\boxed{P}$
5. Return $(\alpha, \beta, \kappa) \in \boxed{P}$ that minimizes $|1 - (L(\alpha)/L(\beta))/R|$

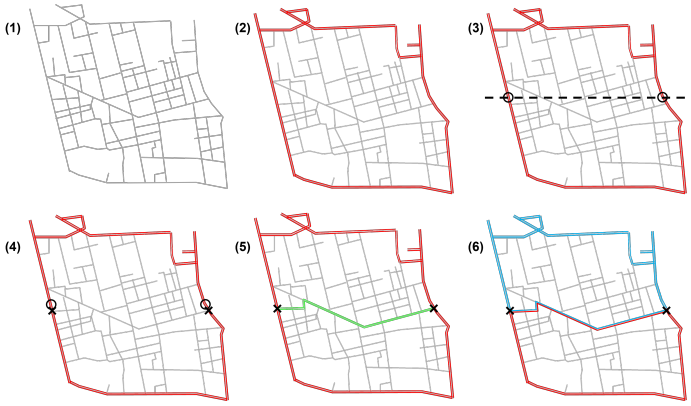

Figure 6: (1) The initial street network; (2) The perimeter of the street network identified through Algorithm A1; (3) A horizontal divider and the pierce points where it crosses the perimeter; (4) The pierce points and the nearest perimeter nodes; (5) The shortest path on the road network between the two perimeter nodes; (6) The perimeters of the two regions produced from the proposed cut

This page intentionally left blank.

APPENDIX D: SARCOP DATA DICTIONARY

SARCOP Data Dictionary

Search/Human Interactions that Do Not Need Follow Up (By Default)		
	Searched Per Rules of Engagement (ROE)	This is a search that has been completed on a structure, vehicle, debris, or other site with no victims or survivors found.
	Rescued	Technical rescue that required moving survivor to a safe location utilizing NFPA 1006 (or equivalent) skillsets such as rope, structural collapse, or swiftwater rescue.
	Evacuated	Survivors transported to collection point or out of harm's way.
	Assisted	Materials assistance provided to residents.
	Shelter in Place	Survivors have chosen to remain at current location.
	Human Remains Removed	Human remains removed from specific location.
	Animal Evacuation	Evacuation or rescue of pets / companion animals.

Search/Human Interactions that Need Follow Up (By Default)		
	Victim Detected	Potential live survivor detected (including canine alert or intelligence).
	Victim Confirmed	Confirmed live survivor (visual, audible, physical confirmation) requiring NFPA 1006 (or equivalent) skillsets such as rope, structural collapse, or swiftwater rescue.
	Human Remains Detected	Potential human remains detected (including canine alert or intelligence).
	Human Remains Confirmed	Confirmed human remains (visual or physical confirmation).
	Targeted Search	Specific location that will require increased search effort (e.g., a 911 phone call, missing person report, etc.).

Damage Observations		
	Unaffected	No visible or reported damage.
	Affected	Damage to the structure is mostly cosmetic.
	Minor	Repairable non-structural damage.
	Major	Structural damage or other significant damage that requires extensive repairs.
	Destroyed	The structure is a total loss.
	Unknown	The status of the structure is unknown.

Additional damage observation guidance can be found here: flood damage, non-flood damage, PDA Pocket Guide.

Updated for v9 SARCOP on April 28, 2023

SARCOP Data Dictionary

Hazards		
	Animal Hazard	Animal hazard related to aggression, location, or disease.
	Fire Incident	General fire occurrence.
	Hazardous Material Incident	Nuclear, biological, or chemical incident
	Flood/Water Level	Current location of water line.
	Route Blocked	Inaccessible route by land or water.
	Other Hazard	Other hazard not already identified.

Other/Incident Support		
	Situation Update	Used to provide a general situation update to include Conditions, Actions, Needs, and Location as needed. team.
	Lifeline Report	Report of status or issue affecting the continuous operation of critical government and business functions essential to human health and safety or economic security. Community lifelines are broken into: Safety and Security; Food, Water, Shelter; Health and Medical; Energy; Communications; Transportation; Hazardous Material. More Info
	Casualty Collection Point	Location that is used for the assembly, triage (sorting), medical stabilization and evacuation of casualties. CCP must account for the rescued and provide for their needs, including medical care, tracking, shelter, food, and more.
	Extra 21	Mission specific placeholder to be determined.
	Extra 22	Mission specific placeholder to be determined.
	Extra 23	Mission specific placeholder to be determined.
	Extra 24	Mission specific placeholder to be determined.
	Aerial hazard*	A hazard for aircraft, such as towers and power lines.
	Airstrip or Airport*	Any area of land or water used or intended for landing or takeoff of aircraft.
	Helispot*	A natural or improved takeoff and landing area intended for temporary or occasional helicopter use.
	Helibase*	The main location within the general incident area for parking, fueling, maintenance, and loading of helicopters. It is usually located at or near the incident base.
	Medical*	Functional unit that is responsible for the emergency medical and occupational health care of incident personnel.
	Incident Command Post (ICP) *	Location at which primary command functions are executed. The ICP may be collocated with the incident base or other incident facilities.
	Drop Point*	A predefined location where personnel, equipment, and supplies will be delivered or picked up. This can also be used for water access for flood/swiftwater resources.

Updated for v9 SARCOP on April 28, 2023

SARCOP Data Dictionary

	Staging*	Locations set up at an incident where resources can be placed while awaiting a tactical assignment on a three (3) minute available basis. Staging Areas are managed by the Operations Section.
	Internet Access*	A location users can get cellular or Wi-Fi access.
	Repeater*	A radio signal station that automatically relays a radio transmission, sometimes over a different frequency, thereby increasing the range of transmission.
	Safety Zone*	A location that is confirmed to be safe from hazard or threat (e.g., above maximum flood height, clear from wildfire hazard, far from falling debris in an earthquake).
	BoO/Camp*	A geographical site(s), within the general incident area, separate from the incident base, equipped and staffed to provide sleeping, food, water, and sanitary services to incident personnel.
	Other Logistics*	Other logistics not already assigned. An example may be location to access fuel.

*Symbols from the National Wildfire Coordinating Group PMS 936 Symbology Event Points

Tracklog Mission Types		
	Ground Recon	Preliminary survey of the area by ground (How Big and How Bad).
	Aerial Recon	Preliminary survey of the area by air (How Big and How Bad).
	Water Recon	Preliminary survey of the area by water (How Big and How Bad).
	Hasty/Rapid Search	Fast paced and methodical search of the area.
	Primary Search	Quick search of the structures likely to contain victims.
	Secondary Low Coverage Search	Systematic search of every room and void space of every structure in the assigned area of operation. *This is not simply “the second time” searching an area.
	Secondary High Coverage Search	Exhaustive search of every room and void space of every structure in the assigned area of operation. This will include complete de-layering and removal of collapsed debris to ensure thoroughness.
	Targeted Search	Searches of specific locations such as shelter locations, high occupancy locations, critical infrastructure facilities, areas of last refuge, and location of special needs individuals or at-risk persons.
	Canine Search Team Live Find	Search of an area using live find canines.
	Canine Search Team Human Remains Detection	Search of an area using Human Remains Detection canines.
	Damage Observation	Mission to document the severity of damage to structures.

Updated for v9 SARCOP on April 28, 2023

This page intentionally left blank.

REFERENCES

[1] Collins, M. (n.d.). *How Esri's ArcGIS powers key collaboration in search and rescue operations*. Retrieved from geoweeknews: https://www.geoweeknews.com/sponsored/how-esri-s-arcgis-powers-key-collaboration-in-search-and-rescue-operations

[2] Federal Emergency Management Agency. (2018). An Introduction to the Incident Command System, ICS-100. FEMA.

[3] FEMA / New Light Technologies. (n.d.). *TEMPO*. Retrieved from https://tempo.nltmso.com/?bbox=-164.439%2C7.100%2C-26.870%2C61.662

[4] National Alliance for Public Safety GIS. (2023, April 29). *SARCOP Data Dictionary* . Retrieved from National Search and Rescue Geospatial Coorindation Group : https://www.arcgis.com/home/item.html?id=da089975974d45a3826e246be2d10be6

[5] National Public Radio. (2013, July 1). *NPR: The Zip Code Turns 50 Today;Hhere Are 9 That Stand Out*. Retrieved from https://www.npr.org/sections/thetwo-way/2013/07/01/197623129/the-zip-code-turns-50-today-here-are-9-that-stand-out

[6] National Technolody and Development Program, USFS. (n.d.). Retrieved from https://www.fs.usda.gov/t-d/nwcg/

[7] US Census Bureau. (n.d.). *Glossary*. Retrieved from US Census Bureau : https://www.census.gov/programssurveys/geography/about/glossary.html#:~:text=Block%20Groups%20(BGs)%20are%20statistical,data%20and%20control%20block%20numbering.

[8] Wisoncisn Department of Transportation. (n.d.). *Production Rate Table*. Retrieved from https://wisconsindot.gov/Documents/doing-bus/eng-consultants/cnslt-rsrces/tools/estimating/production-rate-table.pdf